

TI Designs

Smart Lock Reference Design with Extended Flash Memory Enabling More Than Five Years of Life on Four AA Batteries



Description

With the increasing number of building and home owners looking to retrofit smart locks (or electronic locks) to their buildings or homes, wireless battery-powered smart locks are becoming increasingly popular in today's market. In a smart lock application, the high-current motor and radio often drain the battery quickly, causing battery life to suffer. Replacing multiple batteries can be a time-consuming and costly issue, therefore lowering the average current consumption is often a key design consideration.

Resources

TIDA-00757	Design Folder
DRV8833	Product Folder
CC2640R2F	Product Folder
TPS62745	Product Folder
LP55231	Product Folder
CSD25310Q2	Product Folder
TPD1E10B06	Product Folder

Features

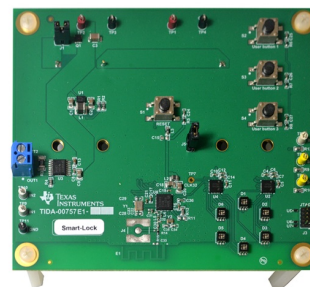
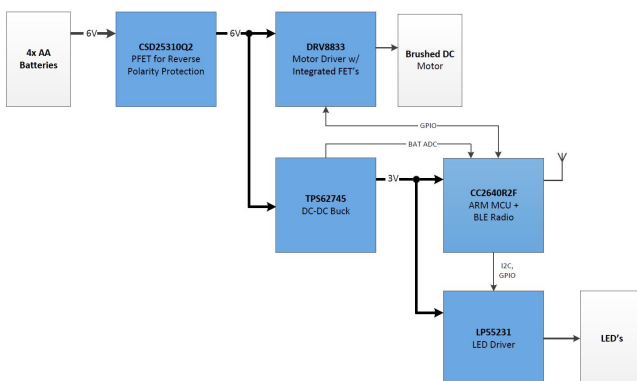
- Five Years of Battery Life Using Four AA Batteries
- Ultra-Low-Power Consumption:
 - Total Average Current Consumption of 58.2 μA (24 Locks and Unlocks Per Day)
 - 4.6- μA Standby Current
 - 61 μA / MHz Arm[®] Cortex[®]-M3
 - DC/DC Converter Uses 33.4 μA of Average Power (500-ms Advertisement Interval)
- Integrated *Bluetooth*[®] Radio and MCU for Smaller Form Factor
- Motor Driver Has Integrated FETs and Current Sense Comparator, Enabling Easy Design and Small Solution Size With Minimal Discretes
- Configurable Advertisement Interval up to 4 Seconds

Applications

- Electronic Smart Lock
- Door Keypads and Readers
- Building Automation
- Building Security Systems
- HVAC Valve and Actuator Control



ASK Our E2E[™] Experts



An IMPORTANT NOTICE at the end of this TI reference design addresses authorized use, intellectual property matters and other important disclaimers and information.

1 Key System Specifications

Table 1. Key System Specifications

PARAMETER	SPECIFICATION	DETAILS
Input power source	Four AA alkaline batteries (operating range from 3.7 V to 6.4 V)	See Section 8.1.1
Bluetooth low energy advertisement interval	500 ms	See Section 8.2
Average Bluetooth low energy and MCU current consumption	26- μ A average (24-hour period)	See Section 8.2
Average losses of power topologies (by design)	LDO: 366.9 μ W	See Section 3.2
	Buck: 30.7 μ W	
	Boost: 349.9 μ W	
Lock or unlock events	24 events per day	
Motor type	Brushed DC	See Section 7.3
Motor current	50-mA average (2-A peak)	See Section 8.4.4
Motor drive without LEDs	45-mA average (per event, 2 seconds)	See Section 8.4.4
Motor drive with LEDs	50-mA average (per event, 2 seconds)	See Section 8.5.1
	27.8- μ A average (per day, 24 events)	
User interface	3 buttons, 6 RGB LEDs	See Section 2.6
Total system power consumption	58- μ A average (with LEDs)	See Section 8.5.4
Estimated battery life	5.29 years	See Section 8.5.5
Test results	5.0 V, 25 C, 24 events, 500 ms	See Section 8

2 System Description

With the increasing number of building and home owners looking to retrofit smart locks (or electronic locks) to their building or home, wireless battery-powered smart locks have become increasingly popular in today's market. In a smart lock application, the high-current motor and radio often drains the battery quickly, causing battery life to suffer. Replacing multiple batteries can be a timely and costly issue, therefore lowering the average current consumption is often a key design consideration. Enabled by TI's light load efficient DC/DC converter, SimpleLink™ ultra-low-power wireless MCU platform, integrated motor driver, and RGB LED driver, this design guide demonstrates how a light load efficient power topology can increase battery life based on low standby current and long off-state intervals. This design guide addresses component selection, design theory, and test results of the TI Design system. The scope of this design guide gives system designers a head-start in implementing a low-power door lock design for electronic locks, door keypads and readers, wireless automatic blinds, and HVAC dampers and actuators.

The following subsections describe the various blocks within the TI Design system and which characteristics are most critical to best implement the corresponding function.

2.1 Battery Choice

Batteries were chosen for two main reasons: capacity and popularity of the battery platform. AA batteries have a greater capacity than AAA batteries. Also, at the time of this writing, AA batteries are used in more applications similar to the smart lock in the present-day market.

2.2 Reverse Polarity Protection

Figure 1 shows the reverse polarity protection.

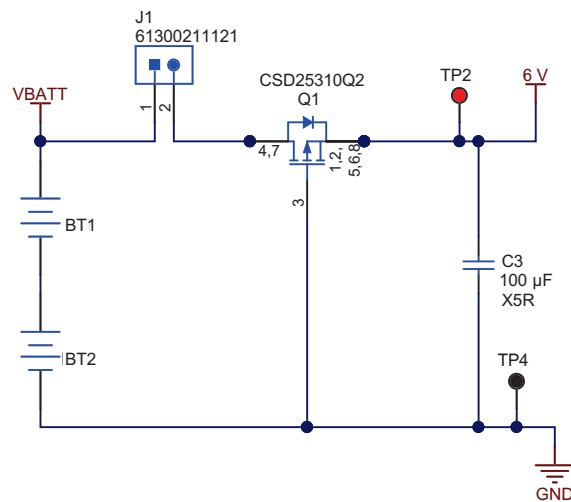


Figure 1. Battery Polarity Protection

A PFET or an NFET can be used to protect against reverse polarity protection. However, a PFET was used in this reference design because the PFET does not break up the ground circuit as an equivalent NFET circuit does.

2.2.1 Using a FET

The most recent MOSFETs are very low resistance and therefore ideal for providing reverse current protection with minimal loss. [Figure 2](#) shows a low-side NMOS FET in the ground return path, and [Figure 3](#) shows a high-side PMOS FET in the power path.

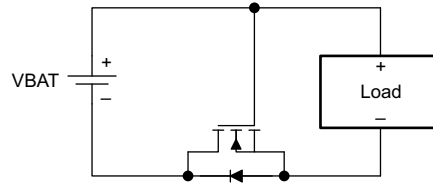


Figure 2. NMOS FET Ground Return Path

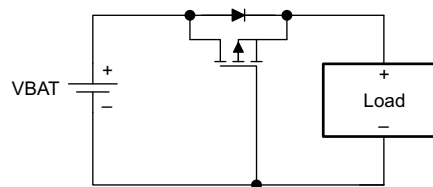


Figure 3. PMOS FET Power Path

In each circuit, the body diode of the FET is oriented in the direction of normal current flow. When the battery is installed incorrectly, the NMOS (PMOS) gate voltage of the FET is low (high), preventing it from turning on. When the battery is installed properly and the portable equipment is powered, the NMOS (PMOS) gate voltage of the FET is taken high (low), and its channel shorts out the diode

A voltage drop of $r_{DS(on)} \times I_{LOAD}$ is seen in the ground return path when using the NMOS FET, and in the power path when using the PMOS FET. In the past, the primary disadvantage of these circuits has been the high cost of low $r_{DS(on)}$, low-threshold voltage FETs. However, advances in semiconductor processing have resulted in FETs which provide minimal drops in small packages.

2.3 Power Topologies

Three main power topologies are possible for this smart lock applications: low drop-out (LDO) regulator, step-down converter (also known as buck), and boost (see [Figure 4](#)). The LDO and buck implementations are not event dependent, meaning the two topologies use the same amount of energy regardless of how many lock and unlock events occur in a day. The LDO and buck drop the voltage down to generate the lower voltage power rail to run the MCU, and the higher voltage components are run off the higher battery voltage. The boost is event dependent because each lock and unlock event must boost up the voltage from 3 V to 5 V for motor and LED operation.

A buck configuration was chosen because the LDO has ground leakage current, whereas the buck has zero ground leakage current and therefore more efficiency. More analysis into power topologies is covered in [Section 3.2](#).

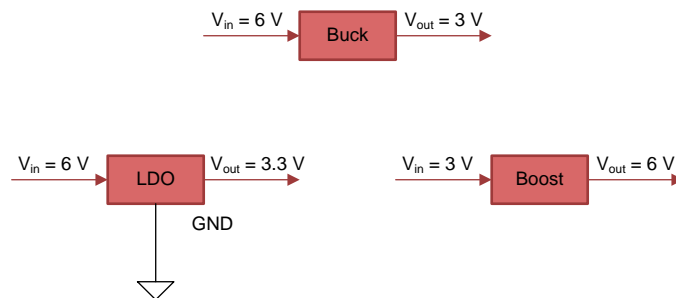


Figure 4. Power Topologies

The TPS62745 step-down converter was chosen because of the extra benefits it offers for low-power designs. This TPS device has select lines which allow the user to select the output voltage, and therefore removes the need for a feedback resistor. The BOM cost can be decreased slightly because there is no feedback resistor. The TPS62745 can dynamically enable or disable the battery voltage check with the use of an enable pin and external resistor voltage divider. Energy is conserved because the voltage divider is only enabled when a battery voltage check is necessary. The rest of the time the divider circuitry does not use energy and is not connected. The TPS62745 is also efficient at extremely light loads; it is 85% efficient at 10 μ A.

2.4 MCU With Integrated Bluetooth® low energy Radio

This reference design must connect and communicate with a central device. However, because power consumption is a concern in battery-based applications, the radio and processor must be low power. Also, the wireless protocol required for the end-equipment system is an important consideration for the selection of the radio device. With TI's SimpleLink ultra-low-power wireless MCU platform, low power with a combined radio and MCU enables extremely long battery life for sensor end nodes. Furthermore, the CC2650 device is a multi-standard device, targeting ZigBee®, 6LoWPAN, and ZigBee RF4CE remote control applications.

2.5 Motor Driver

Drive current, power-supply voltage range, load motor types, and safety shutdown functions were all factors when choosing a motor driver. The DRV8833 includes all of the necessary features. The DRV8833 can drive many types of motors and inductive loads, with a peak current of 2 A and a power-supply voltage range of 2.7 V to 10.8 V, making it ideal to run off of four AA batteries. The nominal drive voltage is 5 V from the batteries. The major discriminating factor of the DRV8833 is the ability to clamp the current at a certain level determined by the external resistor. The DRV8833 has a current-sense function which allows the driver to monitor and adjust the output current so the motor does not burned out or waste power from the battery. The motor can be protected by setting the DRV8833 current limit below the motor stall current.

2.6 User Interface

The user interface on the board must be simple and low power, yet refined enough to display all the information necessary to know what the device is doing. Six RGB LEDs arranged in a circular pattern were chosen to allow different patterns and colors to communicate what is happening to the user. Patterns and colors are helpful because colors can be indistinguishable for color-blind people. The LP55231 is a 9-channel LED driver, and two of the channels enable the 6 RGB LED implementation previously discussed. If cost is an issue, fewer LEDs can be used with only one LP55231. Other important features of the LP55231 include high-efficiency LED drivers and a charge pump (up to 94%), 200-nA standby current, automatic power-save mode, programmable LED patterns, and a small package size (4 mm × 4 mm). Because this reference design implements two LED drivers, the LP55231 was chosen because it allows simple synchronization with a trigger input.

3 System Design Theory

This design guide uses the CC2640R2F MCU with integrated Bluetooth low energy (BLE) radio device to wirelessly lock and unlock your door while: monitoring the battery voltage for low-life indication, limiting the current through the motor (great for the life of the motor), and communicating these events back to the user through LED lighting and patterns. This design achieves an extremely long battery life through the choice of power topology, in this case a highly-efficient buck converter, the TPS62745, and through the use of extending the duty cycle of the Bluetooth low energy connection events.

There are four main devices in all smart lock systems: the MCU, Bluetooth radio, motor driver, and power management. This design focuses on these four devices (three in this case since the CC2640R2F is an MCU with integrated Bluetooth radio) and their equations used for average power consumption to determine the life of the batteries. Once the average power per device is calculated, then it is possible to calculate the battery life in mW-hours. To calculate the battery life, two different current scenarios are examined:

- When the Bluetooth is on and sending out a connection event every 500 ms (or any other value chosen by the user)
- When a lock or unlock event signals the motor driver to pump around 1 A of current through the DC motor

We are ignoring the time when the Bluetooth is paired, because usually this means an event is about to occur, and the amount of current delivered through the motor is almost two orders of magnitude higher than the current flowing to the Bluetooth device. For the purpose of this guide, an event is either a lock or unlock scenario. For example, if the user unlocks the door and then locks it afterward, that is considered two events (one for the lock event and one for the unlock event).

3.1 Bluetooth® low energy and MCU Connection Interval and Average Power Consumption

Because of this system topology, the CC2640R2F only uses the first current scenario described in Section 3. Figure 5 shows a typical current waveform. The period between connection events can be programmed from 10 ms to 4 s in the Bluetooth stack. The pulse-width of the connection event current (or on current) is at 5 ms.

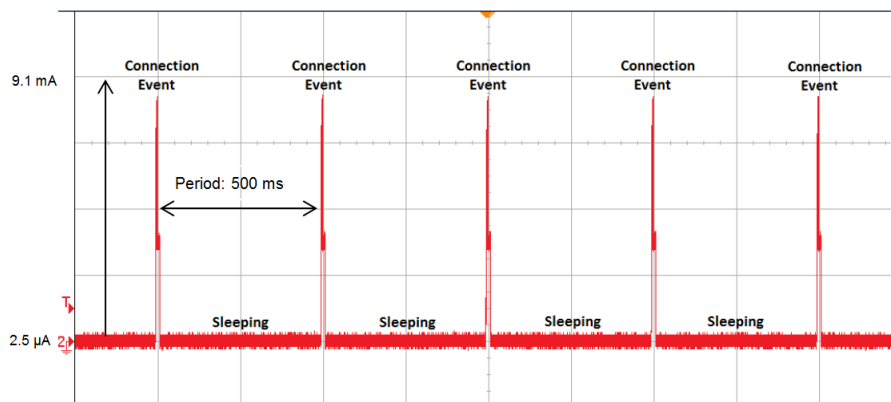


Figure 5. Current Consumption versus Time During Bluetooth® low energy Connections

The main parameters of the Bluetooth and MCU which affect the total estimated battery life are as follows:

- The supply voltage: $V_{\text{supply}} = 3 \text{ V}$
- The on current: $I_{\text{on}} = 9.1 \text{ mA}$
- The off current: $I_{\text{off}} = 2.5 \text{ µA}$
- The on duty cycle: $D_{\text{on}} = t_{\text{on}} / T = 5 \text{ ms} / 500 \text{ ms} = 1\%$
- The off duty cycle: $D_{\text{off}} = 1 - D_{\text{on}} = 99\%$

Equation 1 describes the average power consumed during operation with values taken from their respective data sheets.

$$P_{BLE} = (V_{supply}) \times (I_{on}) \times (D_{on}) + (V_{supply}) \times (I_{off}) \times (D_{off})$$

$$P_{BLE} = (3V) \times (9.1\text{ mA}) \times (0.01) + (3V) \times (2.5\text{ }\mu\text{A}) \times (0.99) = 280.4\text{ }\mu\text{W} \quad (1)$$

The current waveform in Figure 5 occurs until the batteries expires, regardless of how many times the user wirelessly locks or unlocks the door.

3.2 Power Topologies: LDO Versus Buck Versus Boost

A smart lock system can use three different types of power topologies: LDO, buck, and boost. These regulators transfer power from the input to the output. Not all of the power is transferred to the output, some of it is lost. The efficiency of each device is measured by how much of the power is transferred to the output from the input. The LDO and buck topology powers the Bluetooth radio, MCU, and LED drivers, where the motor driver is powered straight from the four AA batteries. The boost topology does the complete opposite and powers the motor driver while the batteries power up the other devices. The voltage of four AA batteries is 6 V, but it only lasts for a short time as seen on alkaline battery life curves. A typical one-cell AA battery (and AAA) usually has a voltage of 1.25 V for the majority of its life. The following equations use this 1.25 V-rating per cell, 5 V for a four-cell battery, because it is a more accurate measurement for average power loss. Both the LDO and buck topology use the 4s1p battery configuration, while the boost configuration uses the 2s2p configuration. Again, the average power equations used in this section are power losses and not power consumed. This section includes power loss equations of all three topologies to better choose a power topology for a smart lock design.

3.2.1 LDO

The main parameters of the LDO regulator that affect the total estimated battery life are:

- The input voltage: $V_{in} = 5\text{ V}$ (four AA batteries in series, nominal voltage)
- The output voltage: $V_{out} = 3\text{ V}$
- The output on current: $I_{on} = 9.1\text{ mA}$
- The output off current: $I_{off} = 5\text{ }\mu\text{A}$
- The ground current: $I_{gnd} = 35\text{ }\mu\text{A}$ (this value could be higher depending on the LDO)
- The on duty cycle: $D_{on} = t_{on} / T = 5\text{ ms} / 500\text{ ms} = 1\%$
- The off duty cycle: $D_{off} = 1 - D_{on} = 99\%$

Equation 2 describes the average power loss of the LDO during operation.

$$P_{LDO} = (V_{in} - V_{out}) \times (I_{on}) \times (D_{on}) + (V_{in} - V_{out}) \times (I_{off}) \times (D_{off}) + (V_{in}) \times (I_{gnd})$$

$$P_{LDO} = (5V - 3V) \times (9.1\text{ mA}) \times (0.01) + (5V - 3V) \times (5\text{ }\mu\text{A}) \times (0.99) + (5V) \times (35\text{ }\mu\text{A}) = 366.9\text{ }\mu\text{W} \quad (2)$$

The I_{off} current is at $5\text{ }\mu\text{A}$ because of the quiescent current of both the BLE device (CC2640R2F) and the LED Driver (LP55231). The I_{gnd} current value can be taken from any LDO regulator data sheet. On some data sheets, this value can also be referred to as the quiescent current. I_{gnd} is the difference between the input current and the output current, and it is a key characteristic for differentiating the efficiency of different LDOs.

3.2.2 Buck

The main parameters of the buck converter that affect the total estimated battery life are:

- The output voltage: $V_{out} = 3\text{ V}$
- The output on current: $I_{on} = 9.1\text{ mA}$
- The output off current: $I_{off} = 5\text{ }\mu\text{A}$
- The efficiency at the on current: $\eta_{on} = 91\%$ (taken from the TPS62745 data sheet)
- The efficiency at the off current: $\eta_{off} = 80\%$ (taken from the TPS62745 data sheet)
- The on duty cycle: $D_{on} = t_{on} / T = 5\text{ msec} / 500\text{ msec} = 1\%$
- The off duty cycle: $D_{off} = 1 - D_{on} = 99\%$

Equation 3 describes the average power loss of the buck converter during operation.

$$P_{Buck} = \left(\frac{1}{\eta_{on}} - 1\right) \times (V_{out}) \times (I_{on}) \times (D_{on}) + \left(\frac{1}{\eta_{off}} - 1\right) \times (V_{out}) \times (I_{off}) \times (D_{off})$$

$$P_{Buck} = \left(\frac{1}{0.91} - 1\right) \times (3\text{ V}) \times (9.1\text{ mA}) \times (0.01) + \left(\frac{1}{0.8} - 1\right) \times (3\text{ V}) \times (5\text{ }\mu\text{A}) \times (0.99) = 30.7\text{ }\mu\text{W} \quad (3)$$

Users can already see that the average power loss in the buck converter is an order of magnitude less than the LDO. The biggest differentiation in buck converters is the efficiency at both current loads, especially at the lighter load of $5\text{ }\mu\text{A}$. Most converters are not as efficient at these lighter loads. The TPS62745 is a highly efficient buck converter, the reason for the choice. The majority of buck converters give their efficiency values on a curve as shown in Figure 6.

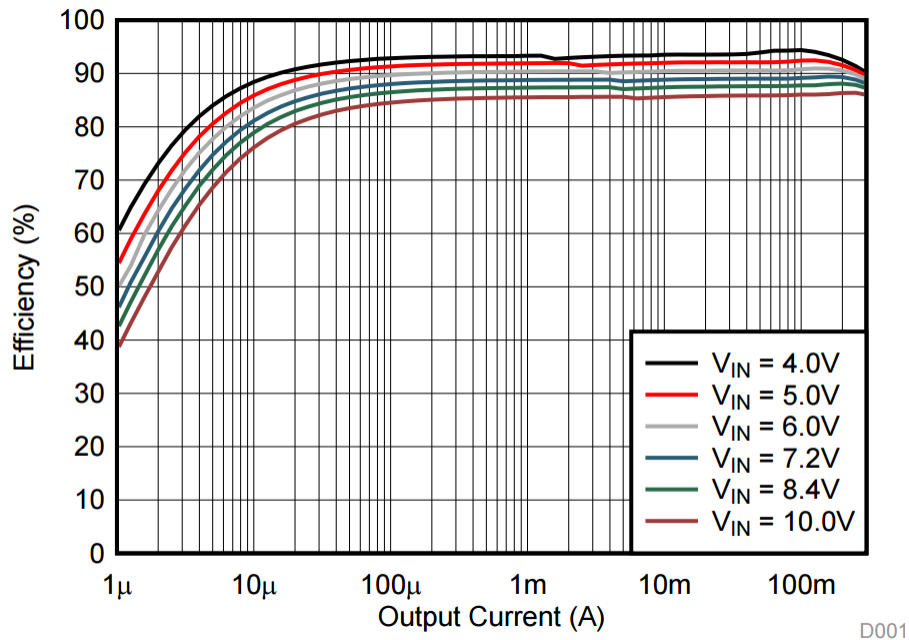


Figure 6. TPS62745 Efficiency Curve at $V_{out} = 3.3\text{ V}$

3.2.3 Boost

The main parameters of the boost converter that affect the total estimated battery life are:

- The output voltage: $V_{out} = 5\text{ V}$
- The average output motor current 1: $I_{out1} = 600\text{ mA}$
- The average output motor current 2: $I_{out2} = 168\text{ mA}$
- The efficiency at I_{out1} : $\eta_1 = 90\%$ (this value could be lower depending on the boost device)
- The efficiency at I_{out2} : $\eta_2 = 85\%$ (this value could be lower depending on the boost device)
- The average number of lock and unlock events per day: $N = 24$ (this number can vary)
- The on time of I_{out1} : $t_{on1} = 2$ seconds (the time when the motor begins to turn)
- The on time of I_{out2} : $t_{on2} = 4$ seconds (the time when braking and reconfiguring the direction of the motor)
- The total period in a day: $T = (3600) \times (24) = 86,400$ seconds

Equation 4 describes the average power loss of the boost converter during operation.

$$P_{Boost} = \left(\frac{1}{\eta_1} - 1\right) \times (V_{out}) \times (I_{out1}) \times \left(\frac{(t_{on1}) \times (N)}{T}\right) + \left(\frac{1}{\eta_2} - 1\right) \times (V_{out}) \times (I_{out2}) \times \left(\frac{(t_{on2}) \times (N)}{T}\right)$$

$$P_{Boost} = \left(\frac{1}{0.9} - 1\right) \times (5\text{ V}) \times (600\text{ mA}) \times \left(\frac{(2) \times (24)}{86400}\right) + \left(\frac{1}{0.85} - 1\right) \times (5\text{ V}) \times (168\text{ mA}) \times \left(\frac{(4) \times (24)}{86400}\right) = 349.9\text{ }\mu\text{W}$$
(4)

The boost configuration is highly dependent on the number of lock and unlock events (N) which occur per day as seen in Equation 4. As the number of lock and unlock events are decreased to 12 (half of 24), the power losses are also cut in half. Because the number of events is directly proportional with power losses, an unfavorable result, the boost is not preferred in a smart E-Lock design when stepping up from 5 V to 6 V from 2.5 V to 3 V.

3.2.4 Power Budget of All Three Power Topologies

The buck converter is by far the topology of choice for this design. Because the majority of the power consumed and lost is in the three main devices (Bluetooth low energy/MCU, power regulator, and motor drive), Figure 7 shows these three and the percentages of how much power is used. The motor driver power consumption and losses are in the next section, but the values are included for visual representation. The PFET for reverse polarity protection is not included in the pie chart because it consumes less than 1% of the total power in all of the following cases. The number of events is 24 for all pie charts. Figure 7 shows the Bluetooth low energy connection period at 500 ms, while Figure 8 shows the Bluetooth low energy connection period at 220 ms (this connection period is sometimes used in different applications like the Apple® HomeKit™).

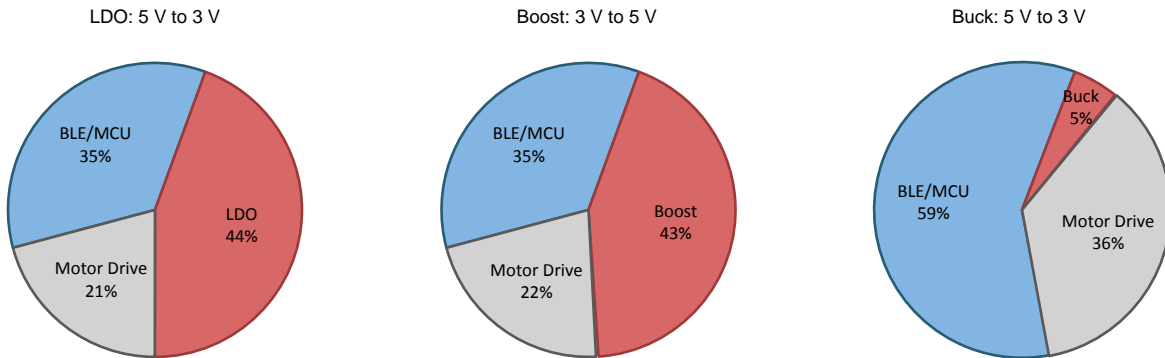


Figure 7. Power Consumption With 500 ms Bluetooth® low energy Connection Period, Using 24 Lock and Unlock Events

With a 500-ms connection period, the system is sleeping or off most of the time. The LDO and boost power configurations take up a significant amount of power (almost half in both cases) compared to the buck configuration, just 6%. Increasing the connection event period (this is an increase in duty cycle) to 220 ms (see Figure 8), shows similar results. In this case, the Bluetooth low energy/MCU consumes more power. The buck configuration is the most ideal power topology by far, as seen in Figure 7 and Figure 8.

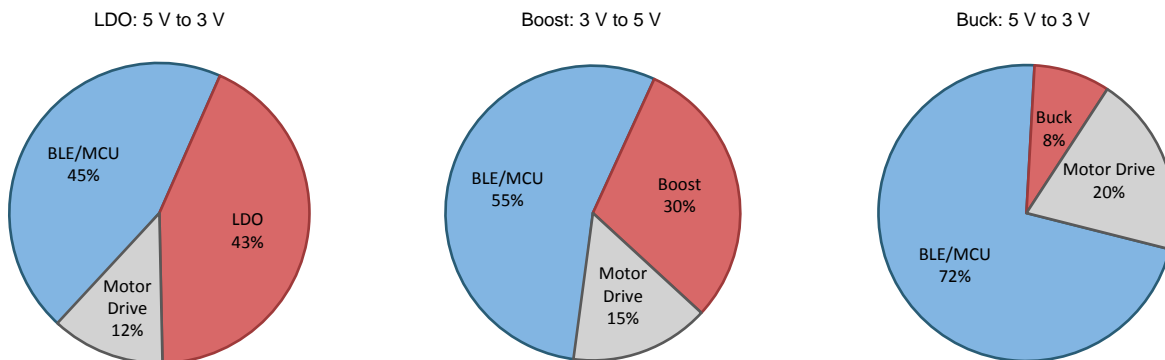


Figure 8. Power Consumption With 220 ms Bluetooth® low energy Connection Period, Using 24 Lock and Unlock Events

3.2.5 Battery Life Versus Number of Lock and Unlock Events of all Three Power Topologies

The following plots show the battery life, in months, versus the number of lock and unlock events per day. The plots provide a better visual representation of why the buck converter is the power topology of choice for battery life. The power dissipation of all the devices (Bluetooth low energy/MCU, PFET, motor driver, and power) are included in the following graphs. The equations used in [Section 3.2](#) were incorporated into all the graphs. [Figure 9](#) shows the battery life with a 500-ms Bluetooth low energy connection period, whereas [Figure 10](#) shows the battery life with a 220-ms Bluetooth low energy connection period.

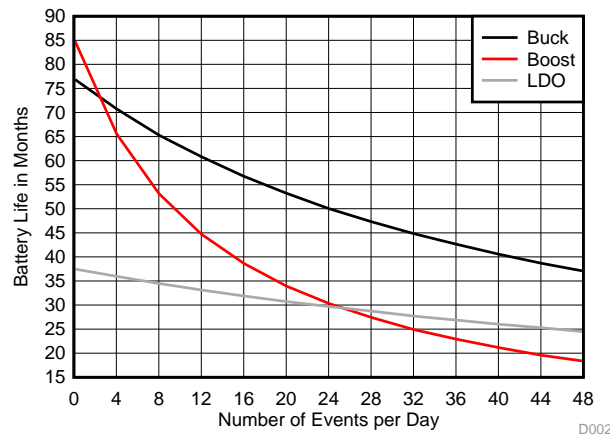


Figure 9. Number of Events Versus Battery Life With 500-ms *Bluetooth*[®] low energy Connections

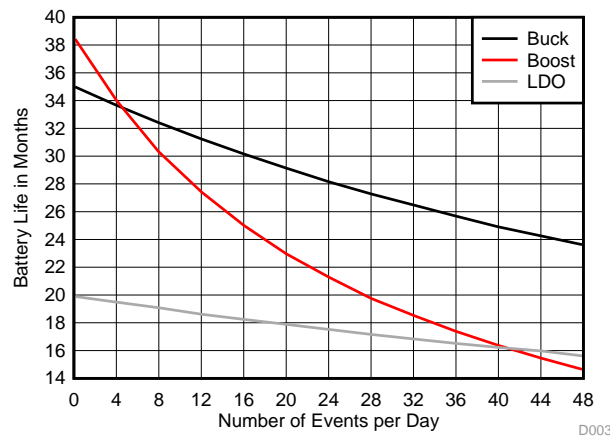


Figure 10. Number of Events Versus Battery Life With 220-ms *Bluetooth*[®] low energy Connections

Another method to extend battery life is to extend the Bluetooth low energy connection period. The CC2640R2F can be programmed to extend the connection period from 10 ms to 4 seconds. Some products, like the Apple HomeKit, have strict connection specifications. Figure 11 shows the battery life versus the period of Bluetooth low energy connections using 12 lock and unlock events, whereas Figure 12 shows the same graph, but this time using 24 lock and unlock events. With the increase of lock and unlock events, the buck topology becomes more advantageous than the other power topologies, as seen in Figure 12.

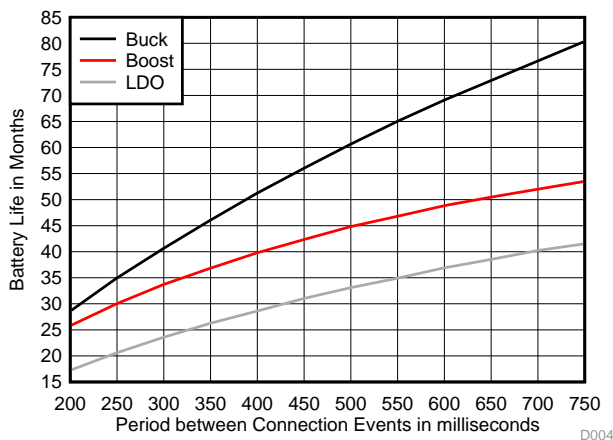


Figure 11. Bluetooth® low energy Connection Period Versus Battery Life With 12 Events

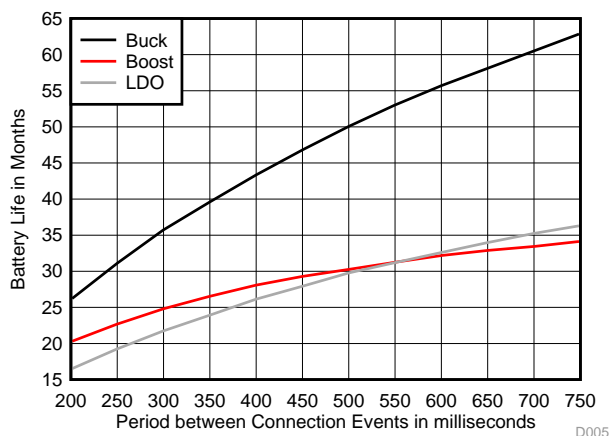


Figure 12. Bluetooth® low energy Connection Period Versus Battery Life With 24 Events

3.3 Motor Driver Average Power Consumption

A number of sources of power dissipation exist inside a motor driver IC. To make an accurate assessment of the total power dissipation, all sources must be considered. The motor driver in this design (DRV8833) has a current-sense pin which limits the amount of the current through the H-bridge and motor. The sense resistor also dissipates power on top of the other sources. In all, there are four sources of power dissipation in a motor driver application (more exist, but the power dissipated in them is negligible and therefore does not make a significant difference in the overall equation). For a more in depth explanation on calculating motor driver power dissipation, see [Calculating Motor Driver Power Dissipation](#).

3.3.1 R_{DSon} Dissipation

The biggest source of power dissipated inside a motor driver device is the power dissipated in the FET on resistance, R_{DSon}. Similar to the boost power topology section, two current scenarios are at play: when the motor begins to turn and when it is coasting and braking.

The main parameters of R_{DSon} dissipation which affect the total estimated battery life follow.

- The on resistance of the H-bridge FETs: $R_{DSon} = 360 \text{ m}\Omega$ (DRV8833 data sheet)
- The root mean square current 1: $I_{RMS1} = 447 \text{ mA}$ (this is different from average current)
- The root mean square current 2: $I_{RMS2} = 140 \text{ mA}$

Equation 5 shows the power dissipated through the on resistance of the FETs during operation.

$$P_{Rds1} = (R_{DSon}) \times (I_{RMS1})^2$$

$$P_{Rds1} = (360 \text{ m}\Omega) \times (0.447 \text{ A})^2 = 71.93 \text{ mW}$$

$$P_{Rds2} = (R_{DSon}) \times (I_{RMS2})^2$$

$$P_{Rds2} = (360 \text{ m}\Omega) \times (0.14 \text{ A})^2 = 7.06 \text{ mW}$$

(5)

3.3.2 Switching Losses

The main parameters of switching losses which affect the total estimated battery life follow.

- The supply voltage: $V_M = 5 \text{ V}$
- The average output motor current 1: $I_{M1} = 600 \text{ mA}$
- The average output motor current 2: $I_{M2} = 168 \text{ mA}$
- The frequency that the output is switching: $f_{sw} = 50 \text{ kHz}$ (DRV8833 data sheet)
- The rise and fall times of the output: $t_{rise} + t_{fall} = 340 \text{ nsec}$ (DRV8833 data sheet)

Equation 6 shows the switching losses of the H-bridge FETs during operation.

$$P_{SW1} = (1/2) \times (V_M) \times (I_{M1}) \times (f_{SW}) \times (t_{rise} + t_{fall})$$

$$P_{SW1} = (1/2) \times (5 \text{ V}) \times (600 \text{ mA}) \times (50 \text{ kHz}) \times (340 \text{ ns}) = 25.5 \text{ mW}$$

$$P_{SW2} = (1/2) \times (V_M) \times (I_{M2}) \times (f_{SW}) \times (t_{rise} + t_{fall})$$

$$P_{SW2} = (1/2) \times (5 \text{ V}) \times (168 \text{ mA}) \times (50 \text{ kHz}) \times (340 \text{ ns}) = 7.14 \text{ mW}$$

(6)

3.3.3 Operating Supply Current

The main parameters of the operating supply current which affect the total estimated battery life follow.

- The supply voltage: $V_M = 5 \text{ V}$
- The supply current: $I_M = 1.7 \text{ mA}$ (DRV8833 data sheet)
- The sleep current: $I_{MQ} = 1.6 \text{ }\mu\text{A}$ (DRV8833 data sheet)

Equation 7 shows the power consumed through the motor drive device.

$$P_M = (V_M) \times (I_M)$$

$$P_M = (5 \text{ V}) \times (1.7 \text{ mA}) = 8.5 \text{ mW}$$

$$P_{MQ} = (V_M) \times (I_{MQ})$$

$$P_{MQ} = (5 \text{ V}) \times (1.6 \text{ }\mu\text{A}) = 8.0 \text{ }\mu\text{W}$$

(7)

3.3.4 Sense Resistor Dissipation

The sense resistor is used for current regulation. The maximum trip current is set according to the equation in the DRV8833 data sheet. The main parameters of sense resistor power dissipation which affect the total estimated battery life follow.

- The sense resistor: $R_{\text{sen}} = 100 \text{ m}\Omega$
- The root mean square current 1: $I_{\text{RMS1}} = 447 \text{ mA}$ (this is different from average current)
- The root mean square current 2: $I_{\text{RMS2}} = 140 \text{ mA}$

Equation 8 shows the power dissipated through the sense resistor during operation.

$$P_{\text{sen1}} = (R_{\text{DSon}}) \times (I_{\text{RMS1}})^2$$

$$P_{\text{sen1}} = (100 \text{ m}\Omega) \times (0.447 \text{ A}) = 19.98 \text{ mW}$$

$$P_{\text{sen2}} = (R_{\text{DSon}}) \times (I_{\text{RMS2}})^2$$

$$P_{\text{sen2}} = (100 \text{ m}\Omega) \times (0.14 \text{ A}) = 1.96 \text{ mW}$$

(8)

3.3.5 Total Average Power Dissipation

There are two H-bridges in the DRV8833, each connected in parallel to the brushed DC motor. Because of these H-bridges, there is a factor of 2 on the R_{DSon} dissipation and switching losses component of the overall motor driver system. The main parameters of the overall motor driver power dissipation which affect the total estimated battery life follow.

- The on time 1: $t_{\text{on1}} = 2$ seconds (the time when the motor begins to turn)
- The on time 2: $t_{\text{on2}} = 4$ seconds (the time spent braking, coasting, and reconfiguring the direction of the motor)
- The average number of lock and unlock events per day: $N = 24$ (this number can vary)
- The total period in a day: $T = (3600) \times (24) = 86,400$ seconds

Equation 9 shows the average power dissipation in the motor driver overall during operation.

$$P_{\text{MD}} = (2 \times P_{\text{Rds1}} + 2 \times P_{\text{SW1}} + P_{\text{M}} + P_{\text{sen1}}) \times \left(\frac{t_{\text{on1}} \times (N)}{T} \right) + (2 \times P_{\text{Rds2}} + 2 \times P_{\text{SW2}} + P_{\text{M}} + P_{\text{sen2}}) \times \left(\frac{t_{\text{on2}} \times (N)}{T} \right) + P_{\text{MQ}}$$

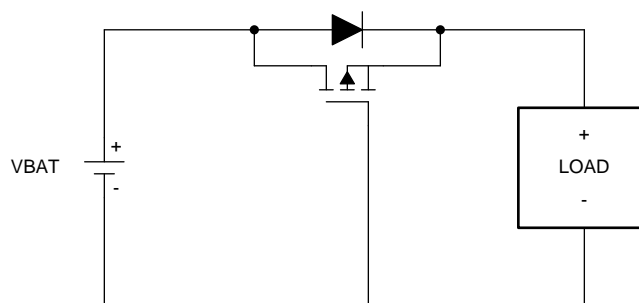
$$P_{\text{MD}} = (2 \times 71.93 \text{ mW} + 2 \times 25.5 \text{ mW} + 8.5 \text{ mW} + 19.98 \text{ mW}) \times \left(\frac{(2) \times (24)}{86400} \right) + (2 \times 7.06 \text{ mW} + 2 \times 7.14 \text{ mW} + 8.5 \text{ mW} + 1.99 \text{ mW}) \times \left(\frac{(4) \times (24)}{86400} \right) + 8 \mu\text{W} = 175.26 \mu\text{W}$$

(9)

The power dissipation on the motor drive device is almost directly proportional to the number of lock and unlock events. Besides using all of the previous equations, a plot of battery life versus the number of events is shown in Section 3.6 to quickly calculate the estimated battery life in months. The experimental average current values are discussed in Section 8.

3.4 Reverse Polarity Protection Power Consumption of PFET

Any system that is powered by batteries must have some kind of safeguard in case of reverse battery installation. If reverse battery installation occurs, there could be serious damage to the internal electronics without a reverse polarity protection circuit. In the theme of ultra-low-power consumption, this design has a PFET, instead of a diode, for its very low on resistance and drop in voltage. The reason for using a PFET instead of a NFET is to prevent breaking the ground plane. The NFET is in the ground return path while the PFET is in the power path. Figure 13 shows how the PFET is wired in the overall circuit.



Copyright © 2016, Texas Instruments Incorporated

Figure 13. Reverse Polarity Protection PFET Configuration

In the circuit in [Figure 13](#), the body diode of the PFET is oriented in the direction of normal current flow. When the battery is installed incorrectly, the gate voltage of the PFET is high, preventing it from turning on. When the battery is installed properly, the gate voltage of the PFET is taken low, and its channel shorts out the diode.

The most important parameter to consider when choosing a PFET is the value of the R_{DSon} (lower is better). The value of the gate charge is not important because this application does not use the PFET as a switching component, and therefore does not have switching losses. The main parameters of the PFET which affect the total estimated battery life follow.

- The on resistance of the PFET: $R_{DSon} = 18 \text{ m}\Omega$ (CSD25310Q2 data sheet)
- The output on current through the PFET: $I_{on} = 6 \text{ mA}$ (current in from battery to buck converter)
- The output off current through the PFET: $I_{off} = 3.75 \text{ }\mu\text{A}$ (current in from battery to buck converter)

The remainder of the parameters are the same as those previously discussed, as follows:

- The on duty cycle: $D_{on} = t_{on} / T = 5 \text{ ms} / 500 \text{ ms} = 1\%$
- The off duty cycle: $D_{off} = 1 - D_{on} = 99\%$
- The average output motor current 1: $I_{out1} = 600 \text{ mA}$
- The average output motor current 2: $I_{out2} = 168 \text{ mA}$
- The on time 1: $t_{on1} = 2 \text{ seconds}$ (time when the motor begins to turn)
- The on time 2: $t_{on2} = 4 \text{ seconds}$ (time spent braking, coasting, and reconfiguring direction of the motor)
- The average number of lock and unlock events per day: $N = 24$ (this number can vary)
- The total period in a day: $T = (3600) \times (24) = 86,400 \text{ seconds}$

[Equation 10](#) shows the average power dissipation in the PFET during operation.

$$P_{PFET} = (R_{DSon}) \times (I_{on})^2 \times (D_{on}) + (R_{DSon}) \times (I_{off})^2 \times (D_{off}) + (R_{DSon}) \times (I_{out1})^2 \times \left(\frac{t_{on1} \times (N)}{T}\right) + (R_{DSon}) \times (I_{out2})^2 \times \left(\frac{t_{on2} \times (N)}{T}\right)$$

$$P_{PFET} = (18 \text{ m}\Omega) \times (6 \text{ mA})^2 \times (0.01) + (18 \text{ m}\Omega) \times (3.75 \text{ }\mu\text{A})^2 \times (0.99) + (18 \text{ m}\Omega) \times (600 \text{ mA})^2 \times \left(\frac{(2) \times (24)}{86400}\right) + (18 \text{ m}\Omega) \times (168 \text{ mA})^2 \times \left(\frac{(4) \times (24)}{86400}\right) = 4.17 \text{ }\mu\text{W}$$
(10)

The current coming in from the battery (I_{on} and I_{off}) was calculated by using the efficiency of the buck converter and then back calculating the input power, hence the input current (5 V is the nominal battery voltage). Looking at the value in [Equation 10](#), 4.17 μW is less than 1% of the total power consumed and lost in this design. The PFET makes an insignificant difference in the overall power budget and battery life.

3.5 Total System Power Consumption

To calculate the total system average power consumption, simply add all average power values from each device from the previous sections (minus the LDO and boost). [Equation 11](#) reflects this combination and shows the total system average power dissipation during operation.

$$P_{avg} = P_{BLE} + P_{Buck} + P_{MD} + P_{PFET}$$

$$P_{avg} = 280.4 \text{ }\mu\text{W} + 30.7 \text{ }\mu\text{W} + 175.26 \text{ }\mu\text{W} + 4.17 \text{ }\mu\text{W} = 490.53 \text{ }\mu\text{W} \text{ (total average power)}$$
(11)

As stated in the beginning of this design guide, these equations only cover the core of any smart lock design. If more peripherals are added to this system, calculate the average power consumed by each extra peripheral by using similar previous methods. For example, determining the duty cycle, calculating the on and off current consumption per peripheral, and so on.

3.6 Theoretical Estimated Battery Life

The majority of batteries show their capacity measured in mA-hours (mAh). The mAh is a measure of current capacity and not really energy capacity (but they are closely related). A better unit for measuring energy capacity of a battery is in milliWatt-hours (mWh). To convert the mAh capacity of a battery to mWh, first look at the battery data sheet.

Take the AA Energizer® battery for example, shown in Figure 14.

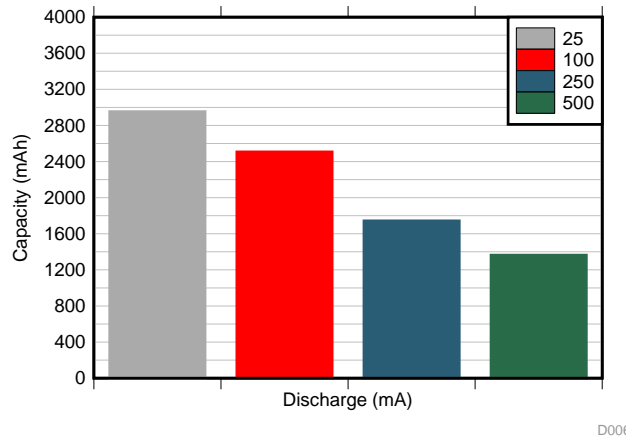


Figure 14. mAh Capacity of Energizer® AA Battery

Calculate the average discharge current in your smart lock system. In this case, the average load current is much less than 25 mA, so look at the capacity at that value (which is the lowest value on the battery data sheet). Then use these parameters to figure out the values needed for total energy capacity of the batteries:

- The battery current capacity of one cell: $I_{\text{energy}} = 3000 \text{ mAh}$ (alkaline AA battery data sheet)
- The number of batteries configured in parallel: $\text{Batt}_{\parallel} = 1$ (all four batteries are in series: 4s1p)
- The number of batteries configured in series: $\text{Batt}_{\text{series}} = 4$
- The starting voltage of one battery cell: $V_{\text{batt}} = 1.5 \text{ V}$ (one alkaline AA battery)

See Equation 12 to convert the batteries current capacity, mAh, into mWh.

$$E_{\text{total}} = (I_{\text{energy}}) \times (\text{Batt}_{\parallel}) \times (V_{\text{batt}}) \times (\text{Batt}_{\text{series}})$$

$$E_{\text{total}} = (3,000\text{mA} - \text{h}) \times (1) \times (1.5\text{V}) \times (4) = 18,000\text{mW} - \text{hours} \tag{12}$$

Lastly, the amount of battery life in hours can be calculated by using the equations in Equation 11 for average power of the system and Equation 12 for total energy capacity of the battery.

Equation 13 shows the number of months of battery life during operation.

$$\text{Months} = \left(\frac{E_{\text{total}}}{P_{\text{avg}}} \right) \times \left(\frac{1 \text{ day}}{24 \text{ hours}} \right) \times \left(\frac{1 \text{ month}}{30.5 \text{ days}} \right)$$

$$\text{Months} = \left(\frac{18,000 \text{ mW} - \text{hours}}{0.49053\text{mW}} \right) \times \left(\frac{1 \text{ day}}{24 \text{ hours}} \right) \times \left(\frac{1 \text{ month}}{30.5 \text{ days}} \right) = 50.1 \text{ months of battery life (5 years)} \tag{13}$$

The final plot shows the battery life, in months, versus the number of lock and unlock events per day using just the buck topology, which is the power topology of choice for this reference design. The plot, shown in [Figure 15](#), shows four different Bluetooth low energy connection event periods on the same graph: 220 ms, 360 ms, 500 ms, and 640 ms. The power dissipation of all devices (Bluetooth low energy/MCU, PFET, motor driver, and power) is included in this MATLAB graph. The equations used in [Section 3](#) were incorporated into all the graphs.

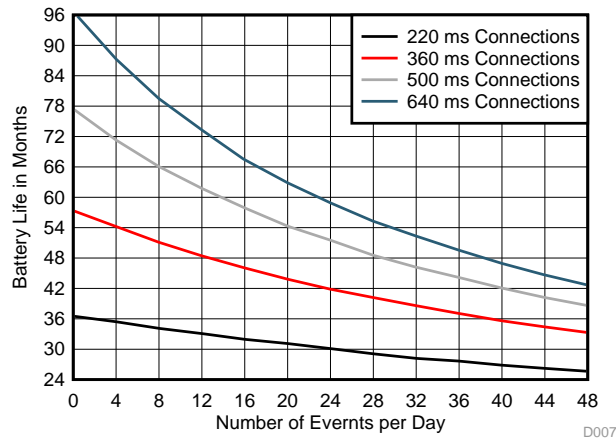


Figure 15. Number of Events Versus Battery Life With Buck Converter

3.7 Firmware Control

TIDA-00757
Software Flow Chart

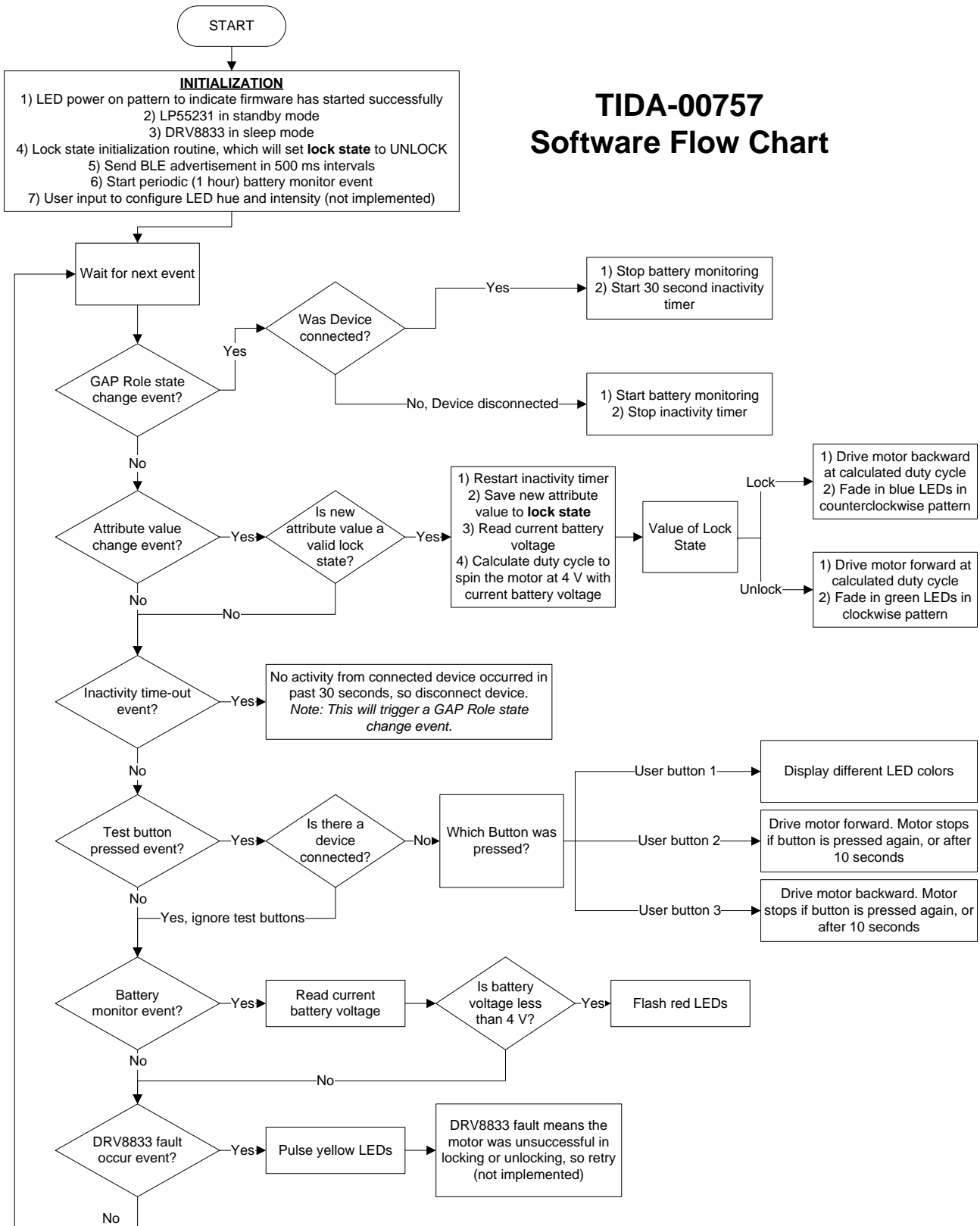


Figure 16. Software Flow Chart

This flow chart shown in [Figure 16](#) describes the CC2640R2F operation in this TI Design. The CC2640R2F starts by initializing and configuring the LP55231 and DRV8833 devices to its lowest power state. Afterward, the CC2640R2F advertises with a 500-ms interval. The CC2640R2F also monitors the battery voltage in 1 hour intervals while it is waiting for a device to connect. The main loop of the CC2640R2F is event based. The majority of the time, the CC2640R2F is in standby mode, except when it must transmit an advertisement packet or check the battery voltage. When an event is triggered, the CC2640R2F wakes up and executes functions depending on the event source.

The CC2640R2F has six event triggers:

- **GAP role state change event:** This event occurs when the GAP role state changes (for example, when a device connects or disconnects from the CC2640R2F). When a device connects to the CC2640R2F, the current load changes. The voltage-based battery monitoring does not give an accurate representation of the battery voltage, because the measured voltage is a function of the battery impedance and the load current. Also, for security and battery savings, a device must not be connected indefinitely. In this firmware, the device is automatically disconnected after 30 seconds of inactivity. When a device connects, the battery monitor is stopped and the inactivity timer is started immediately. When a device disconnects (either by the user or by the inactivity time-out), the battery monitoring resumes.
- **Attribute value change event:** This event occurs when the user changes the lock state. The CC2640R2F first starts by verifying whether the new value is valid. If the new value is not valid, then the value is discarded and no action is taken. If the new value is valid, the lock state is saved and the inactivity timer is restarted. Next, the battery voltage is read to calculate the correct PWM duty cycle to run the motor at 4 V. If the new value is *lock*, the motor drives backward for 1.8 seconds while the blue LEDs turn in a counter clockwise pattern for 2 seconds. If the new value is *unlock*, the motor drives forward for 1.8 seconds while the green LEDs turn in a clockwise pattern for 2 seconds.
- **Inactivity time-out event:** If the 30 second inactivity time-out expires, the CC2640R2F disconnects the device and returns to the advertising. When this event occurs, the CC2640R2F also triggers a GAP role state change event.
- **Test button pressed event:** The test buttons are valid only when a device is not connected. If a device is connected, the test buttons are ignored, so the device does not interfere with the user's operation. If user button *one* is pressed, the CC2640R2F displays different LED colors. If user button *two* is pressed, the CC2640R2F drives the motor forward for a maximum of 10 seconds, or until user button *two* is pressed again. If user button *three* is pressed, the CC2640R2F drives the motor backward for a maximum of 10 seconds, or until the user button *three* is pressed again.
- **Battery monitor event:** This event is the 1 hour battery monitor periodic event. The C2640 reads the current battery voltage. If the battery voltage is less than 4 V, the LEDs flash red.
- **The DRV8833 fault occur event:** If the DRV8833 fault pin indicates an error occurred when running the motor, the LEDs pulse yellow. The current implementation of the firmware only shows a visual indication that a fault occurred. The firmware can be modified to rerun the motor until it can successfully lock or unlock without a fault occurring. In addition, the firmware contains a GATT server with the following services:
 - GAP
 - GATT
 - Device information
 - Lock

Device information service is aligned to official SIG profiles. The lock profile is a custom profile with 128-bit unique UUIDs. The profile enables a device to configure the lock state of the TIDA-00757 TI Design. The complete attribute table for TIDA-00757 is shown in [Table 2](#).

Table 2. TIDA-00757 Attribute Table

HANDLE (HEX)	HANDLE (DEC)	TYPE (HEX)	TYPE (TEXT)	HEX VALUE	GATT SERVER PERMISSIONS	DESCRIPTION AND VALUE (TEXT)
0x1	1	0x2800	GATT Primary Service Declaration	0x1800	R	Generic access service
0x2	2	0x2803	GATT Characteristic Declaration	02:03:00:00:2A	R	Device name
0x3	3	0x2A00	Device Name	—	R	—
0x4	4	0x2803	GATT Characteristic Declaration	02:05:00:01:2A	R	Appearance
0x5	5	0x2A01	Appearance	—	R	—
0x6	6	0x2803	GATT Characteristic Declaration	02:07:00:04:2A	R	Peripheral preferred connection parameters
0x7	7	0x2A04	Peripheral Preferred Connection Parameters	—	R	—
0x8	8	0x2800	GATT Primary Service Declaration	0x1801	R	Generic attribute service
0x9	9	0x2800	GATT Primary Service Declaration	0x180A	R	Device information service
0xA	10	0x2803	GATT Characteristic Declaration	02:0B:00:23:2A	R	System ID
0xB	11	0x2A23	System ID	8B:EF:AD:00:00:84:BE:C4	R	—
0xC	12	0x2803	GATT Characteristic Declaration	02:0D:00:24:2A	R	Model number string
0xD	13	0x2A24	Model Number String	54:49:44:41:2D:30:30:37:35:37:20:54:49:20:44:65:73:69:67:6E	R	TIDA-00757 TI Design
0xE	14	0x2803	GATT Characteristic Declaration	02:0F:00:25:2A	R	Serial number string
0xF	15	0x2A25	Serial Number String	53:65:72:69:61:6C:20:4E:75:6D:62:65:72	R	Serial number
0x10	16	0x2803	GATT Characteristic Declaration	02:11:00:26:2A	R	Firmware revision string
0x11	17	0x2A26	Firmware Revision String	46:69:72:6D:77:61:72:65:20:52:65:76:3A:20:31:2E:30	R	Firmware rev: 1.0
0x12	18	0x2803	GATT Characteristic Declaration	02:13:00:27:2A	R	Hardware revision string
0x13	19	0x2A27	Hardware Revision String	48:61:72:64:77:61:72:65:20:52:65:76:3A:20:31:2E:30	R	Hardware rev: 1.0

Table 2. TIDA-00757 Attribute Table (continued)

HANDLE (HEX)	HANDLE (DEC)	TYPE (HEX)	TYPE (TEXT)	HEX VALUE	GATT SERVER PERMISSIONS	DESCRIPTION AND VALUE (TEXT)
0x14	20	0x2803	GATT Characteristic Declaration	02:15:00:28:2A	R	Software revision string
0x15	21	0x2A28	Software Revision String	53:6F:66:74:77:61: 72:65:20:52:65:76: 3A:20:31:2E:30	R	Software rev: 1.0
0x16	22	0x2803	GATT Characteristic Declaration	02:17:00:29:2A	R	Manufacturer name string
0x17	23	0x2A29	Manufacturer Name String	54:65:78:61:73:20: 49:6E:73:74:72:75: 6D:65:6E:74:73	R	Texas Instruments
0x18	24	0x2803	GATT Characteristic Declaration	02:19:00:2A:2A	R	IEEE 11073-20601 Regulatory Certification Data List
0x19	25	0x2A2A	IEEE 11073-20601 Regulatory Certification Data List	FE:00:65:78:70:65: 72:69:6D:65:6E:74: 61:6C	R	Experimental
0x1A	26	0x2803	GATT Characteristic Declaration	02:1B:00:50:2A	R	PnP ID
0x1B	27	0x2A50	PnP ID	01:0D:00:00:00:10: 01	R	—
0x1C	28	0x2800	GATT Primary Service Declaration	F0007570-0451- 4000-B000- 000000000000	R	Lock service
0x1D	29	0x2803	GATT Characteristic Declaration	0E:1E:00:00:00:00: 00:00:00:00:B0:00: 40:51:04:71:75:00: F0	R	Lock state
0x1E	30	0x7571	Lock State Config	00	RW	Write 0 to unlock, 1 to lock
0x1F	31	0x2901	Characteristic User Description	4C:6F:63:6B:20:53: :74:61:74:65:20:28: 30:3A:55:6E:6C:6F: :63:6B:2C:20:31:3 A: 4C:6F:63:6B:29	R	Lock state (0:unlock, 1:lock)

4 Block Diagram

Figure 17 shows the TIDA-00757 block diagram.

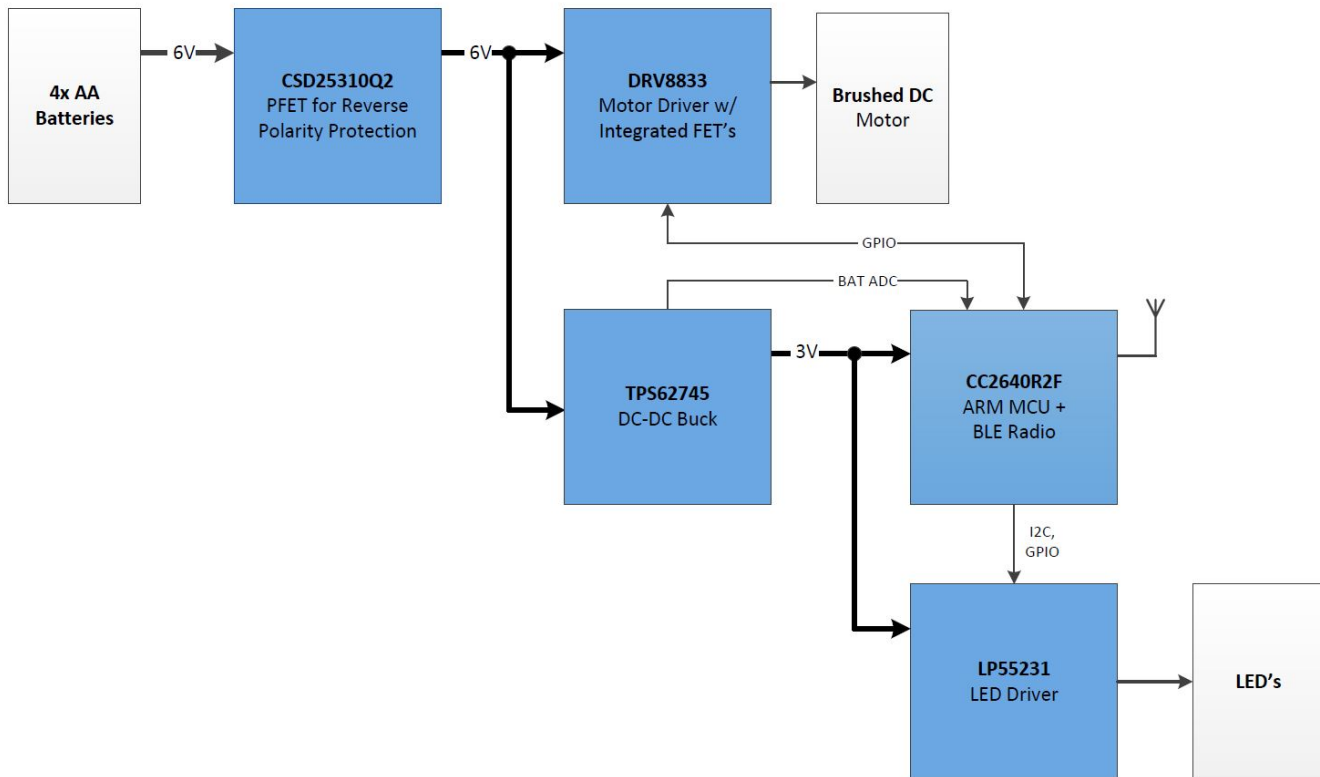


Figure 17. TIDA-00757 Block Diagram

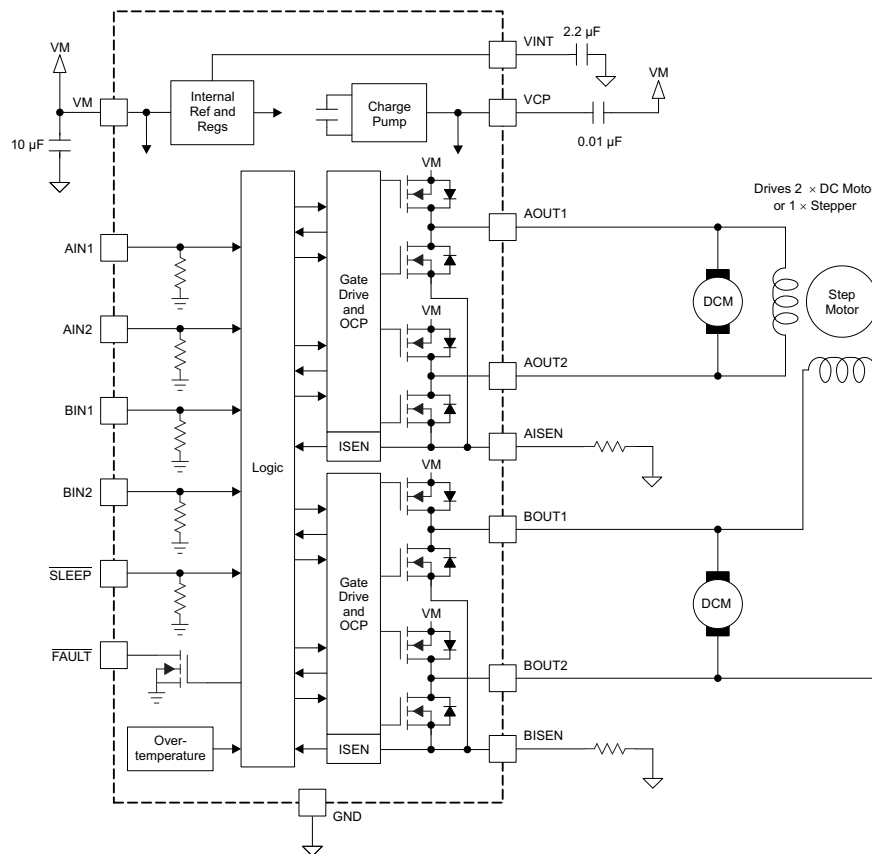
4.1 Highlighted Products

This TI design features the following:

- DRV8833 (Section 4.1.1): Dual H-bridge motor driver with motor current control and low $R_{DS(on)}$ of 360 m Ω
- CC2640R2F (Section 4.1.2): 2.4-GHz Bluetooth low energy with a ultra-low-power wireless MCU (32-bit Arm Cortex-M3 processor)
- TPS62745 (Section 4.1.3): Ultra-low IQ buck converter with 16 selectable output voltages from 1.8 V to 3.3 V and 90% efficiency at load currents $\geq 15 \mu\text{A}$
- LP55231 (Section 4.1.4): Nine-channel LED driver designed to produce lighting effects for mobile devices
- CSD25310Q2 (Section 4.1.5): Low-cost power PFET with gate-to-source voltage of $\pm 8 \text{ V}$ and low $R_{DS(on)}$ of 19 m Ω
- TPD1E10B06 (Section 4.1.6): Single-channel ESD in a 0402 package with 10-pF capacitance and 6-V breakdown

4.1.1 DRV8833

The device has two H-bridge drivers, and can drive two DC brush motors, a bipolar stepper motor, solenoids, or other inductive loads (see Figure 18). The output driver block of each H-bridge consists of N-channel power MOSFETs configured as an H-bridge to drive the motor windings. Each H-bridge includes circuitry to regulate or limit the winding current. Internal shutdown functions with a fault output pin are provided for overcurrent protection, short-circuit protection, undervoltage lockout, and overtemperature. A low-power sleep mode is also provided.



Copyright © 2016, Texas Instruments Incorporated

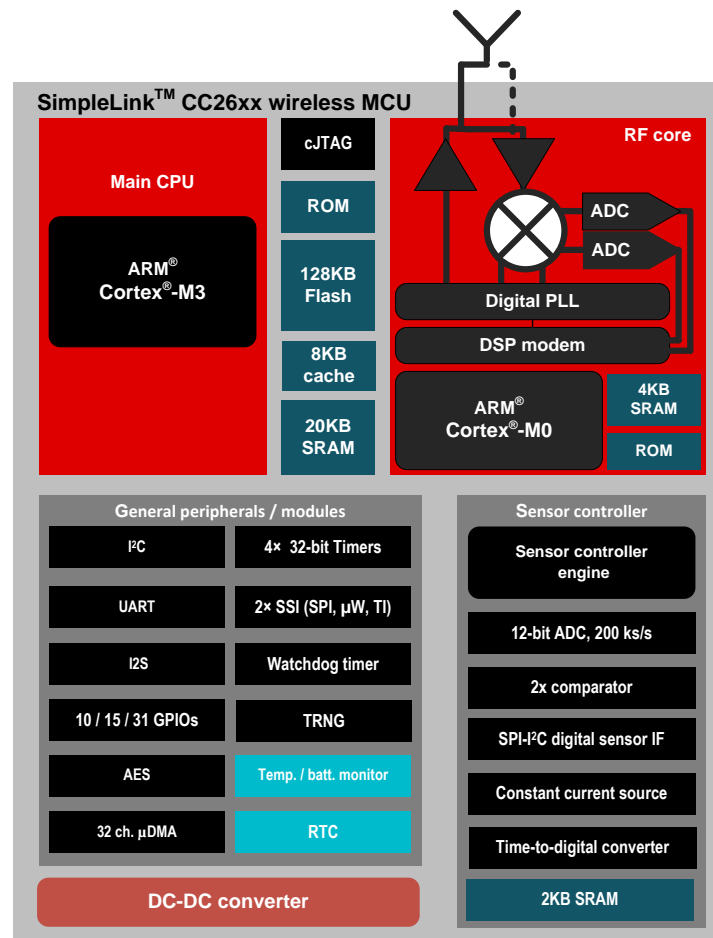
Figure 18. DRV8833 Block Diagram

DRV8833 features:

- Dual H-bridge current-control motor driver
 - Can drive two DC motors or one stepper motor
 - Low MOSFET ON-resistance: HS + LS 360 mΩ
- Output current (at $V_M = 5\text{ V}$, 25°C)
 - 1.5-A RMS, 2-A peak per H-bridge in PWP and RTY package options
 - 500-mA RMS, 2-A peak per H-bridge in PW package option
- Outputs can be in parallel for:
 - 3-A RMS, 4-A peak (PWP and RTY)
 - 1-A RMS, 4-A peak (PW)
- Wide power supply voltage range: 2.7 V to 10.8 V
- PWM winding current regulation and current limiting
- Thermally enhanced surface-mount packages

4.1.2 CC2640R2F

The CC2640R2F device is a wireless MCU targeting Bluetooth applications. The device is a member of the CC26xx family of cost-effective, ultra-low-power, 2.4-GHz RF devices. Very low active RF and MCU current and low-power mode current consumption provide excellent battery lifetime and allow for operation on small coin cell batteries and in energy-harvesting applications. The CC2640R2F device contains a 32-bit Arm Cortex-M3 processor that runs at 48 MHz as the main processor and a rich peripheral feature set that includes a unique ultra-low-power sensor controller (see [Figure 19](#)). This sensor controller is ideal for interfacing external sensors and for collecting analog and digital data autonomously while the rest of the system is in sleep mode. Thus, the CC2640R2F device is ideal for a wide range of applications where long battery lifetime, small form factor, and ease of use is important. The Bluetooth low energy controller is embedded into ROM and runs partly on an Arm Cortex-M0 processor. This architecture improves overall system performance and power consumption and frees flash memory for the application. The Bluetooth stack is available free of charge from TI.com.



Copyright © 2016, Texas Instruments Incorporated

Figure 19. CC2640R2F Block Diagram

CC2640R2F features:

- Microcontroller
 - Powerful Arm Cortex-M3
 - EEMBC CoreMark® score: 142
 - Up to 48-MHz clock speed
 - 128KB of in-system programmable flash
 - 8KB of SRAM for cache
 - 20KB of ultra-low-leakage SRAM

- 2-Pin cJTAG and JTAG debugging
- Supports over-the-air (OTA) upgrade
- Ultra-low-power Sensor Controller
 - Can run autonomous from the rest of the system
 - 16-Bit architecture
 - 2KB of Ultra-low-leakage SRAM for code and data
- Efficient code size architecture, placing drivers, Bluetooth low energy controller, and bootloader in ROM
- RoHS-compliant packages
 - 4-mm × 4-mm RSM VQFN32 (10 GPIOs)
 - 5-mm × 5-mm RHB VQFN32 (15 GPIOs)
 - 7-mm × 7-mm RGZ VQFN48 (31 GPIOs)
- Peripherals
 - All digital peripheral pins can be routed to any gpio
 - Four general-purpose timer modules (eight 16-bit or four 32-bit timers, PWM each)
 - 12-bit ADC, 200-ksamples/s, 8-channel analog MUX
 - Continuous time comparator
 - Ultralow-power analog comparator
 - Programmable current source
 - UART
 - 2× SSI (SPI, MICROWIRE, TI)
 - I²C
 - I2S
 - Real-time clock (RTC)
 - AES-128 security module
 - True random number generator (TRNG)
 - 10, 15, or 31 GPIOs, depending on package option
 - Support for eight capacitive-sensing buttons
 - Integrated temperature sensor
- External system
 - On-chip internal DC/DC converter
 - Very few external components
 - Seamless integration with the SimpleLink CC2590 and CC2592 range extenders
 - Pin compatible with the SimpleLink CC13xx in 4-mm × 4-mm and 5-mm × 5-mm VQFN packages
- Low power
 - Wide supply voltage range
 - Normal operation: 1.8 to 3.8 V
 - External regulator mode: 1.7 to 1.95 V
 - Active-mode RX: 5.9 mA
 - Active-mode TX at 0 dBm: 6.1 mA
 - Active-mode TX at +5 dBm: 9.1 mA
 - Active-mode MCU: 61 μA/MHz
 - Active-mode MCU: 48.5 CoreMark/mA
 - Active-mode sensor controller: 8.2 μA/MHz
 - Standby: 1 μA (RTC running and RAM/CPU retention)
 - Shutdown: 100 nA (wake up on external events)

- RF Section
 - 2.4-GHz RF transceiver compatible with Bluetooth low energy 4.1 specification
 - Excellent receiver sensitivity (–97 dBm for Bluetooth low energy), selectivity, and blocking performance
 - Link budget of 102 dB for Bluetooth low energy
 - Programmable output power up to +5 dBm
 - Single-ended or differential RF interface
 - Suitable for systems targeting compliance with worldwide radio frequency regulations
 - ETSI EN 300 328 (Europe)
 - EN 300 440 Class 2 (Europe)
 - FCC CFR47 Part 15 (US)
 - ARIB STD-T66 (Japan)
- Tools and development environment
 - Full-feature and low-cost development kits
 - Multiple reference designs for different RF configurations
 - Packet sniffer PC software
 - Sensor controller studio
 - SmartRF™ Studio
 - SmartRF Flash Programmer 2
 - IAR Embedded Workbench for Arm
 - Code Composer Studio™

4.1.3 TPS62745

The TPS62745 is a high-efficiency ultra-low-power, synchronous step-down converter optimized for low-power wireless applications. The device provides a regulated output voltage consuming only 400-nA quiescent current. The device operates from two rechargeable Li-Ion batteries, Li-primary battery chemistries such as Li-SOCl₂, Li-SO₂, Li-MnO₂ or four to six cell alkaline batteries. The input voltage range of up to 10 V also allows operation from a USB port and thin-film solar modules. The output voltage is set with four VSEL pins from 1.8 V to 3.3 V for TPS62745 or 1.3 V and 2.8 V for TPS627451. TPS62745 features low output ripple voltage and low noise with a small output capacitor. An internal input voltage switch controlled by pin EN_VIN_SW connects the supply voltage to pin VIN_SW. The switch is intended to be used for an external voltage divider, scaling down the input voltage for an external ADC. The switch is automatically opened when the supply voltage is below the undervoltage lockout threshold. The TPS62745 is available in a small, 12-pin 3 mm × 2 mm WSON package.

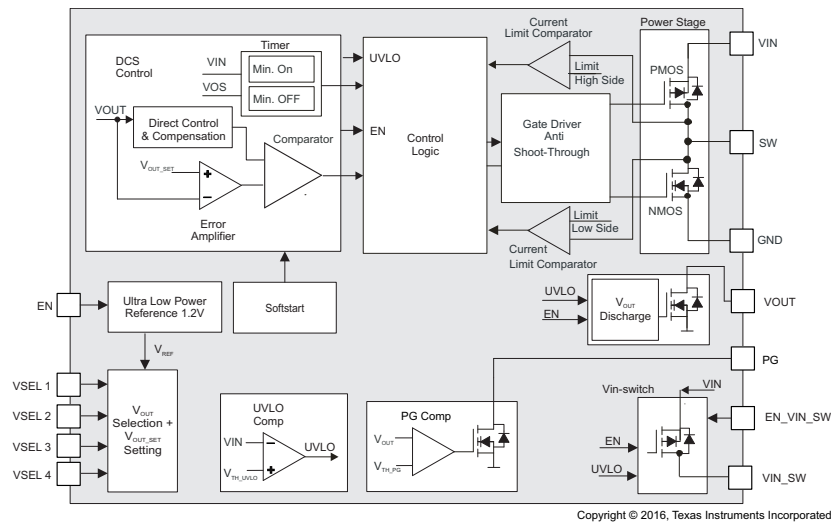


Figure 20. TPS62745 Block Diagram

TPS62745 features:

- Input voltage range VIN from 3.3 V to 10 V
- Typical 400 nA quiescent current
- Up to 90% efficiency with load currents >15 μA
- Up to 300 mA output current
- RF friendly DCS-Control™
- Low output ripple voltage
- 16 selectable output voltages from
 - 1.8 V to 3.3 V (TPS62745)
 - 1.3 V to 2.8 V (TPS627451)
- Integrated input voltage switch
- Integrated discharge function at VOUT
- Open-drain power good output
- Operates with a tiny 3.3-μH or 4.7-μH inductor
- Small 3 mm x 2 mm WSON package

4.1.4 LP55231

The LP55231 is a nine-channel LED driver designed to produce lighting effects for mobile devices. A high-efficiency charge pump enables LED driving over full Li-Ion battery voltage range. The device is equipped with an internal program memory, which allows operation without processor control.

The LP55231 has an I²C-compatible control interface with four pin-selectable addresses. The INT pin can be used to notify the processor when a lighting sequence has ended (interrupt function). Also, the device has a trigger input interface, which allows synchronization, for example, between multiple LP55231 devices. Excellent efficiency is maintained over a wide operating range by autonomously selecting the best charge pump gain based on LED forward voltage requirements. The device can automatically enter power-save mode when LED outputs are not active, thus lowering idle current consumption down to 10 μ A (typical). Only four small and low-cost ceramic capacitors are required.

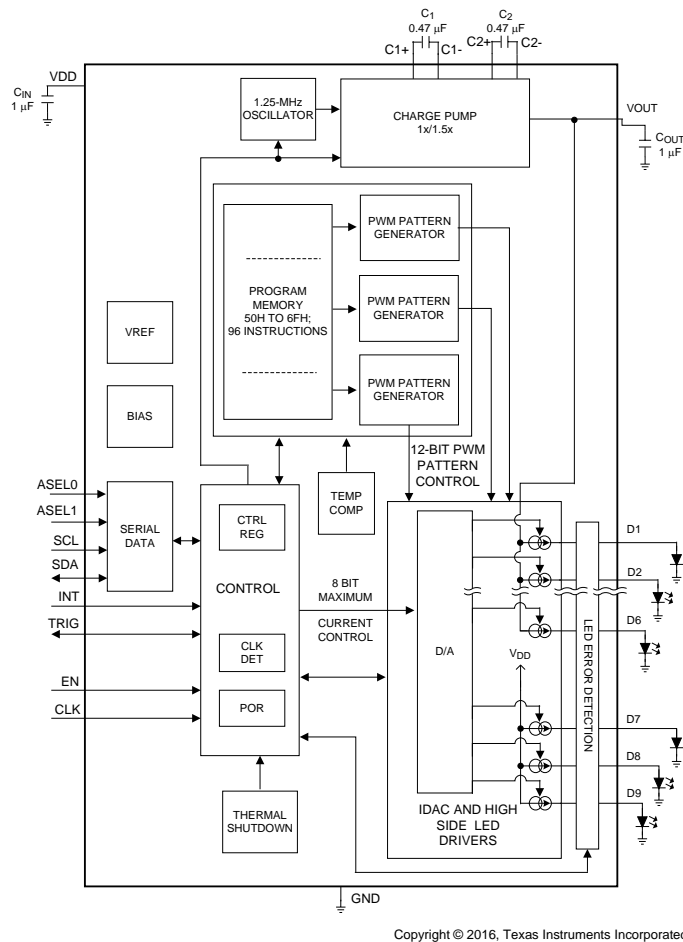


Figure 21. LP55231 Block Diagram

LP55231 features:

- Three independent program execution engines, 9 programmable outputs with 25.5 mA full-scale current, 8-bit current-setting resolution, and 12-bit PWM control resolution
- Adaptive high-efficiency 1x / 1.5x fractional charge pump - efficiency up to 94%
- LED drive efficiency Up to 93%
- Charge pump with soft start and overcurrent and short-circuit protection
- Built-in LED test
- 200-nA typical standby current
- Automatic power save mode; I_{VDD} = 10 μ A (typical)
- Two-wire I²C-compatible control interface

- Flexible instruction set
- Large SRAM program memory
- Small application circuit
- Source (high-side) drivers
- Architecture supports color control

4.1.5 CSD25310Q2

This 19.9-m Ω , -20 V P-channel device is designed to deliver the lowest ON-resistance and gate charge in the smallest outline possible with excellent thermal characteristics in an ultra-low profile. Its low ON-resistance coupled with an extremely small footprint in a SON 2-mm x 2-mm plastic package make the device ideal for battery-operated, space-constrained operations.

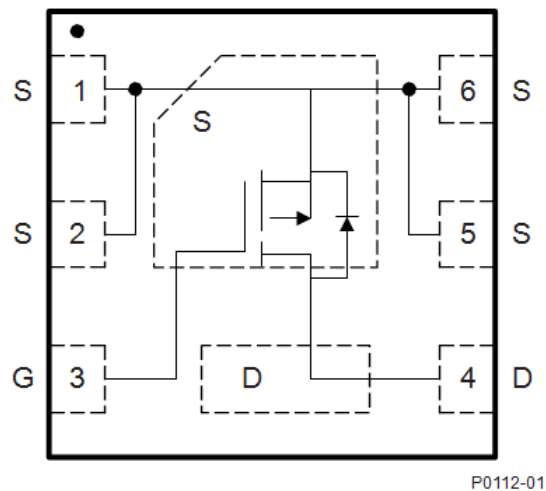


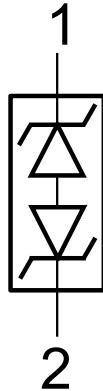
Figure 22. CSD25310Q2 Device Configuration

CSD25310Q2 features:

- Ultra-low Q_g and Q_{gd}
- Low ON resistance
- Low thermal resistance
- Pb-free
- RoHS compliant
- Halogen free
- SON 2-mm x 2-mm plastic package

4.1.6 TPD1E10B06

The TPD1E10B06 device is a single-channel electrostatic discharge (ESD) transient voltage suppression (TVS) diode in a small 0402 package. This TVS protection product offers ± 30 -kV contact ESD, ± 30 -kV IEC air-gap protection, and has an ESD clamp circuit with a back-to-back TVS diode for bipolar or bidirectional signal support. The 12-pF line capacitance of this ESD protection diode is suitable for a wide range of applications supporting data rates up to 400 Mbps. The 0402 package is an industry standard and is convenient for component placement in space-saving applications.



Copyright © 2016, Texas Instruments Incorporated

Figure 23. TPD1E10B06 Block Diagram

TPD1E10B06 features:

- Provides system-level ESD protection for low-voltage I/O interface
- IEC 61000-4-2 level 4 ESD protection
 - ± 30 kV contact discharge
 - ± 30 kV air-gap discharge
- IEC 61000-4-5 surge: 6 A (8/20 μ s)
- I/O capacitance 12 pF (typical)
- R_{DYN} 0.4 Ω (typical)
- DC breakdown voltage ± 6 V (minimum)
- Ultra-low leakage current 100 nA (maximum)
- 10-V clamping voltage (maximum at $I_{PP} = 1$ A)
- Industrial temperature range: -40°C to 125°C
- Space-saving 0402 footprint (1 mm \times 0.6 mm \times 0.5 mm)

5 Getting Started Hardware

This section provides an overview describing how to get started with the EVM hardware.

5.1 Hardware Overview

Figure 24 shows the hardware for the TIDA-00757 reference design. The PCB is in a 3.5-inch x 4.0-inch rectangular form factor. However, no steps were taken to shrink down the form factor during development. The PCB sits on 1-inch nylon standoffs to enable ease of use while performing lab measurements.

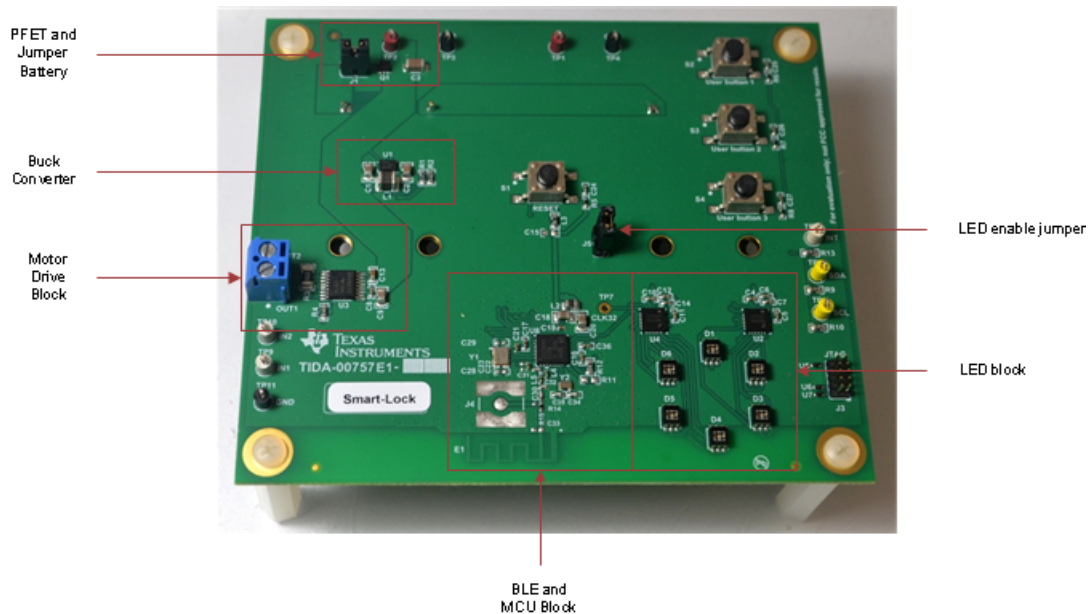


Figure 24. Smart Lock Reference Design Hardware

The board has two jumpers. J1 in the top left corner of the board lets the user disconnect the batteries from the rest of the reference design. J1 also enables collection of current measurements from the 6-V power rail. J5 is near the center of the board and connects the 3-V power rail to the LED drivers. J5 can be useful when the LEDs do not need to be running during testing. The lower left corner of the board contains the motor connection terminal block and test points along with the DRV8833 motor controller. I²C test points and the LED controller interrupt test points are on the lower right corner of the board next to the JTAG programming headers.

The CC2640R2F and PCB antenna are in the lower middle section of the board. Six RGB LEDs are arranged in a circle to the left of the CC2640R2F, with two LP55231 LED controllers positioned above the LEDs. The design also includes a few push buttons. Three user push buttons are in the upper right corner, whereas the reset button is in the middle of the board.

5.2 Operating the Reference Design

TI recommends installing the batteries with J1 removed, and afterwards installing the jumper to power up the circuit. On power up, all six LEDs blink pink to notify the user that the device has powered up correctly (see [Figure 25](#)).

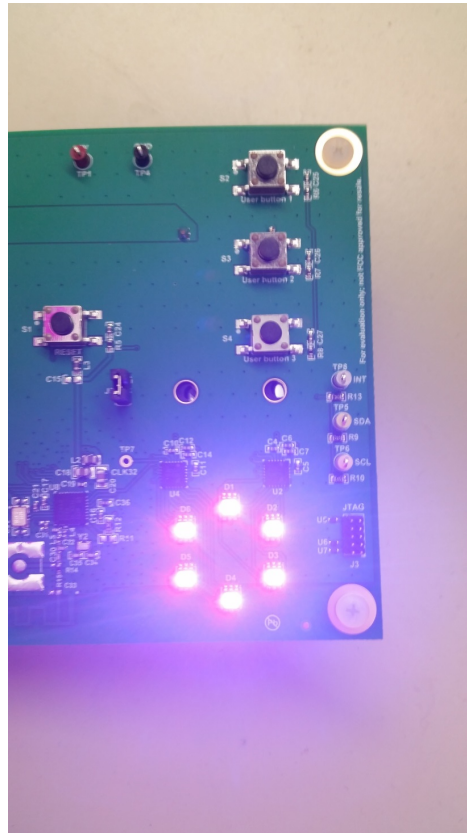


Figure 25. Pink Start-Up LEDs

When a device is not connected using Bluetooth the user buttons (S2, S3, and S4) activate different features of the design. A light show starts when S2 is pressed, and the six RGB LEDs cycle through several different colors. S3 drives the motor forward. The motor stops if S3 is pressed again, or after 10 seconds. S4 drives the motor backward. If S4 is pressed again the motor stops, or after 10 seconds. To communicate using Bluetooth the iOS app called LightBlue™ was used for testing. Other generic Bluetooth apps can be used on various platforms. The B-BLE app on a Samsung® Galaxy S® 6 was tested for functionality. See [Section 6.3](#) for further steps on running the firmware on this reference design.

6 Getting Started Firmware

6.1 Compiling Firmware

The firmware used for this TI Design was developed using TI's CCS software (version 6.1.0), BLE SDK 2.02.00.31, TI-RTOS 2.18.00.03 and Arm Compiler Tools 5.2.7. The instructions to build the firmware assume that CCS and the software packages have been set up and configured correctly. For more information on how to setup the development environment, consult the *CC2640R2F BLE Software Developer's Guide* provided in the docs folder of the BLE SDK.

Importing the CCS Project

1. Open CCS.
2. Click on the *Project* tool bar.
3. Select *Import CCS Projects...*
4. Select the radio option *Select archive file*.
5. Navigate to where the *TIDA00757_BLE_Peripheral_Stack.zip* file was installed. If using the default location, the firmware is at folder location, *C:\ti\TIDA00757-Firmware*
6. Verify that the option *TIDA00757_BLE_Peripheral_Stack* is checked.
7. Click the *Finish* button.
8. Repeat Steps 2 through 7 to import *TIDA00757_BLE_Peripheral_App*

At this point, the CCS workspace should have both *TIDA00757_BLE_Peripheral_App* and *TIDA00757_BLE_Peripheral_Stack* projects.

Building the Firmware

1. Set the *TIDA00757_BLE_Peripheral_Stack* project as the active project, and build the project using *Project* → *Build Project*. The generated binary file, *TIDA00757_BLE_Peripheral_Stack.hex*, is in the *TIDA00757_BLE_Peripheral_Stack/FlashROM* folder.
2. Set the *TIDA00757_BLE_Peripheral_App* project as the active project, and build the project using *Project* → *Build Project*. The generated binary file, *TIDA00757_BLE_Peripheral_App.hex*, is in the *TIDA00757_BLE_Peripheral_App/FlashROM* folder.

6.2 Loading Firmware

The TI Design hardware is programmed by connecting the 10-pin mini ribbon cable from J3 to the SmartRF06 EVM (10-pin Arm Cortex Debug Connector, P410). On the SmartRF06 EVM, set the source switch to *USB*, and short the *VDD to EM* jumper. In this configuration, the SmartRF06 EVM provides power to the CC2640R2F. See the SmartRF06 EVM documentation for more information ([SWRU321](#)).

See [Figure 26](#) for the correct set up for connecting the TI Design hardware to the SmartRF06 EVM. Two applications can be used to program the TIDA-00757: Code Composer Studio or SmartRF Flash Programmer 2.

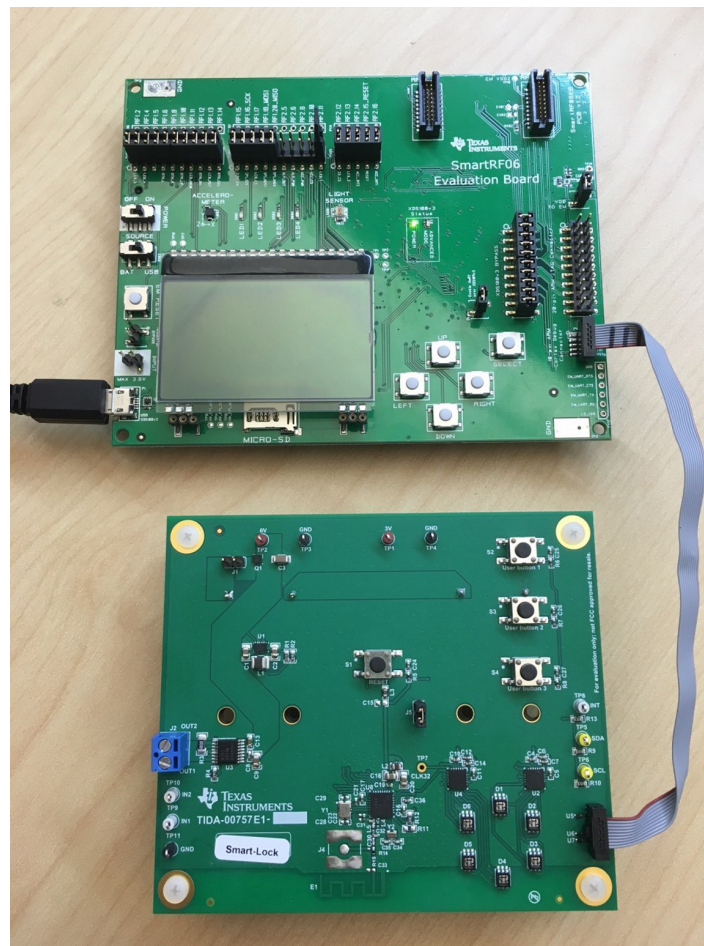


Figure 26. Connection of SmartRF06 Evaluation Board and TI Designs Hardware for Programming and Debugging

6.2.1 Programming With Code Composer Studio™

Perform the following steps to program with CCS:

1. Download *TIDA00757_BLE_Peripheral_Stack* by selecting the *TIDA00757_BLE_Peripheral_Stack* project as the active project, and choosing *Run* → *Debug*.
2. Choose *Run* → *Terminate* to stop the debug.
3. Download *TIDA00757_BLE_Peripheral_App* by selecting the *TIDA00757_BLE_Peripheral_App* project as the active project, and choosing *Run* → *Debug*.

NOTE: The preceding steps are needed only for the initial download, and whenever the Stack project is modified. As long as the Stack project is not modified, the only required steps are:

1. Build the application.
 2. Download the application.
-

6.2.2 Programming With SmartRF™ Flash Programmer 2

Perform the following steps to program with SmartRF Flash Programmer 2:

1. Download and install SmartRF Flash Programmer 2, available at: <http://www.ti.com/tool/flash-programmer>.
2. Open SmartRF Flash Programmer 2.
3. In the *Connected devices* window, CC2640R2F is listed under XDS100v3. If it is not listed, check the power and connection from SmartRF06 to TIDA-00757, and click the *Refresh* button to rescan for devices. Highlight the CC2640R2F device (see [Figure 27](#)).
4. In the *Main* tab, click the *Multiple* radio button.
5. Click the *Browse* button and navigate to the *TIDA00757 Stack hex file*.
6. Click the *Browse* button and navigate to the *TIDA00757 App hex file*.
7. Click the blue circle *Play* button to flash the two hex images onto the TIDA-00757.

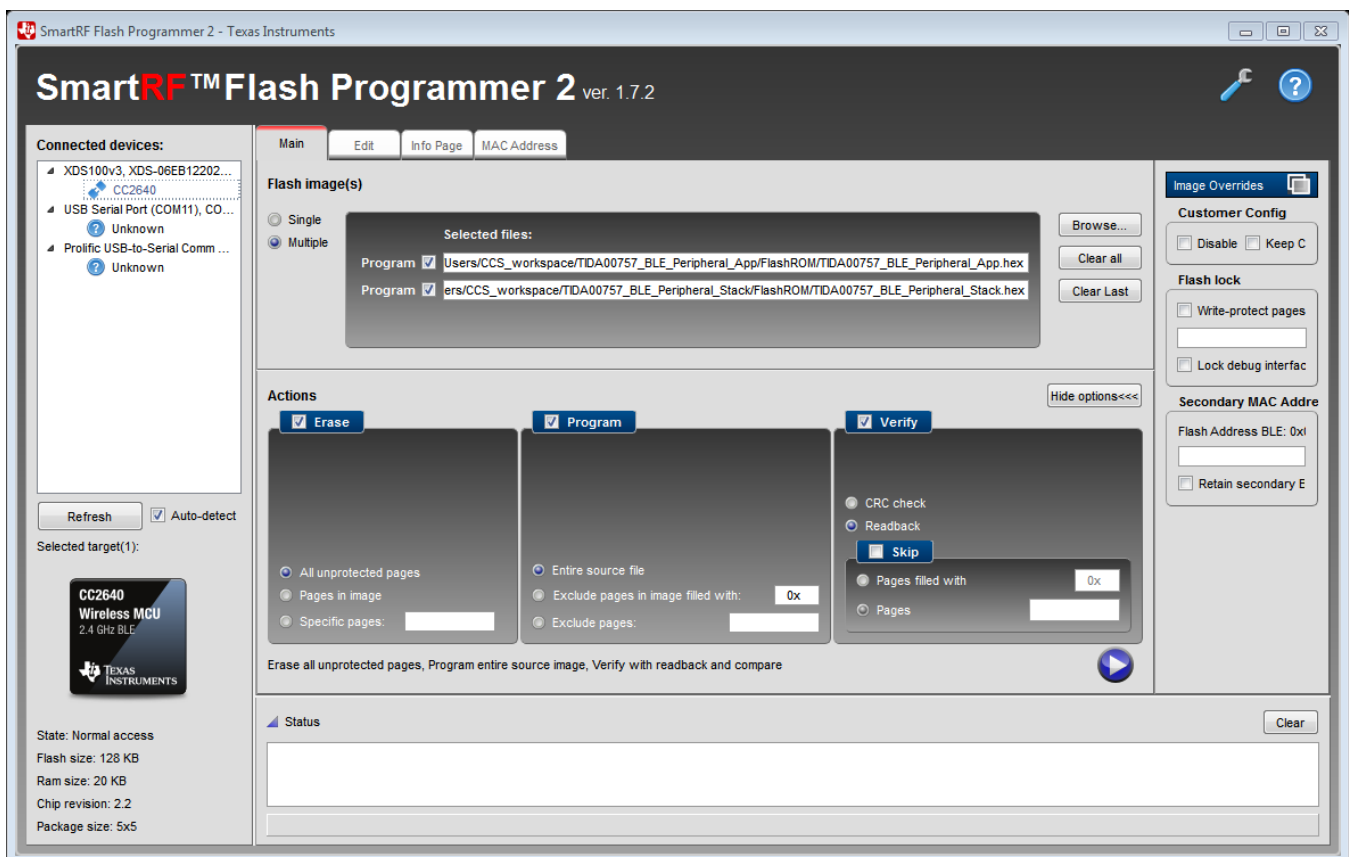


Figure 27. SmartRF™ Flash Programmer 2 Configuration

- The status bar at the bottom of the SmartRF Flash Programmer 2 shows whether flashing the images was successful (see [Figure 28](#)).

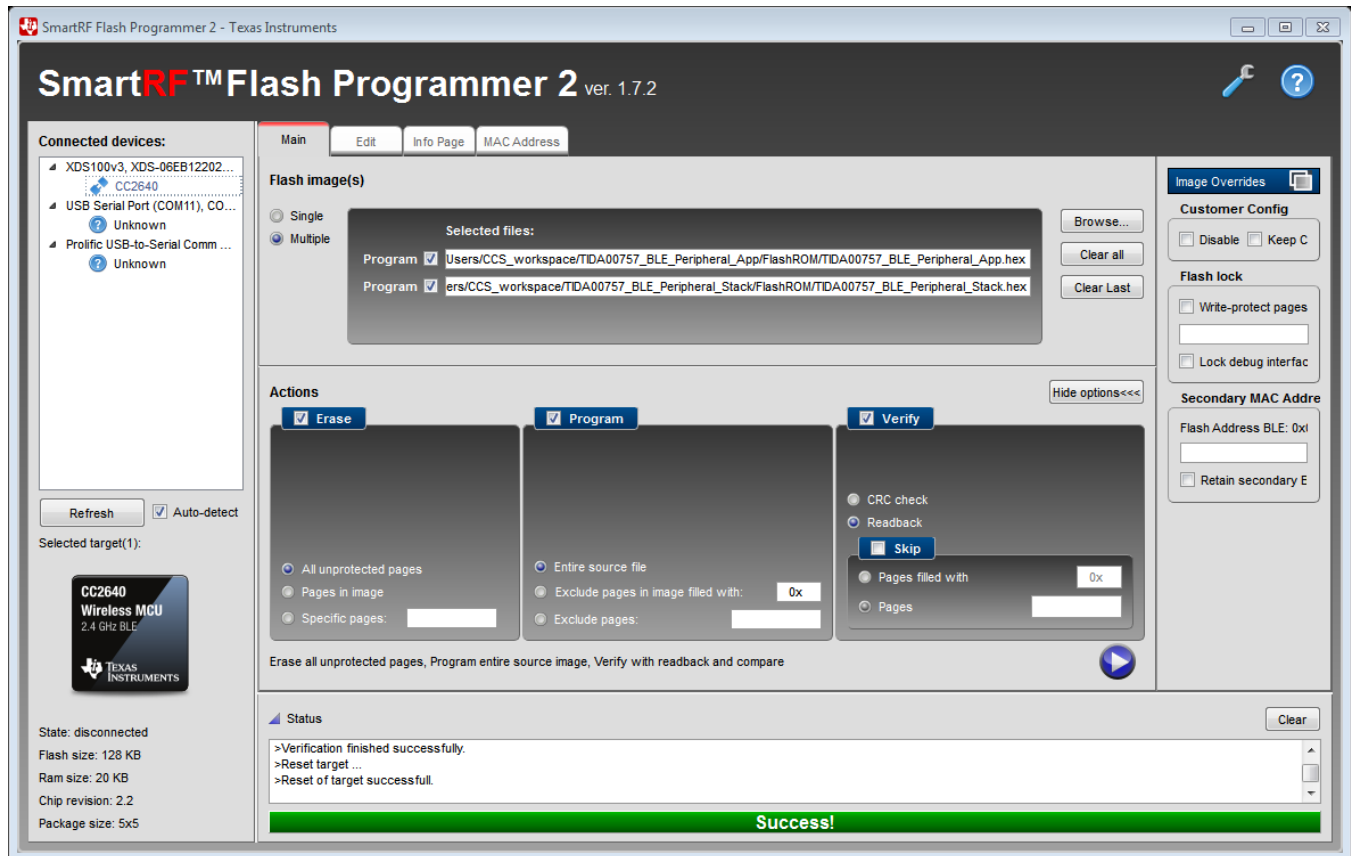


Figure 28. SmartRF™ Flash Programmer 2 Successful Flash Status

6.3 Running Firmware

To communicate with the TIDA-00757, an iPhone 6 with the *LightBlue* iOS app was used for testing. A different platform or app can perform this function. The app *B-BLE* on the Samsung Galaxy S6 was tested for functionality.

- If not previously done, disconnect the SmartRF06 ribbon cable from the TIDA-00757.
- Remove J1 to disconnect the battery from the system.
- Insert four AA batteries into the battery holders or use a bench power supply.
- Power on the board by shunting J1 to connect the battery to the system.

NOTE: The LEDs of the TIDA-00757 flash pink to indicate that the firmware is running.

- Enable Bluetooth on the iPhone
- Run the LightBlue app

7. View the peripherals nearby (see [Figure 29](#)).

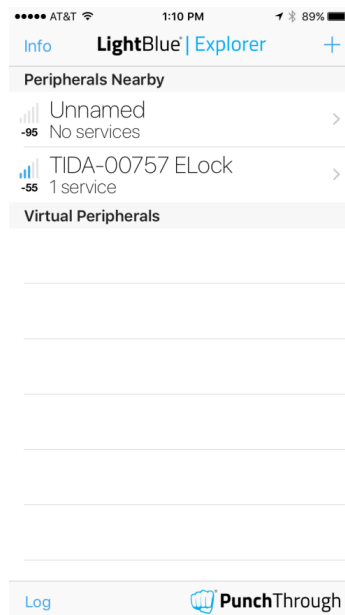


Figure 29. View Peripherals Screen

8. Click the *TIDA-00757 ELock* peripheral to connect (see [Figure 30](#)).

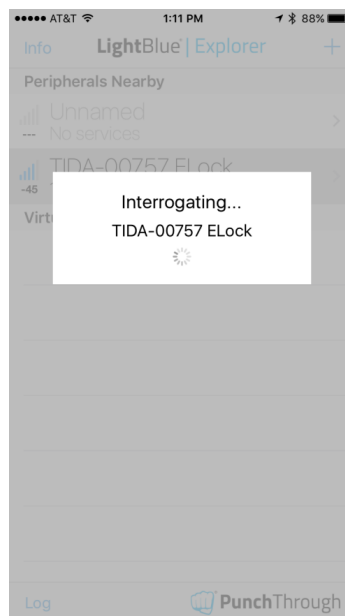


Figure 30. TIDA-00757 Connecting Screen

9. Once connected, the advertisement data and attribute fields can be viewed (see [Figure 31](#)).

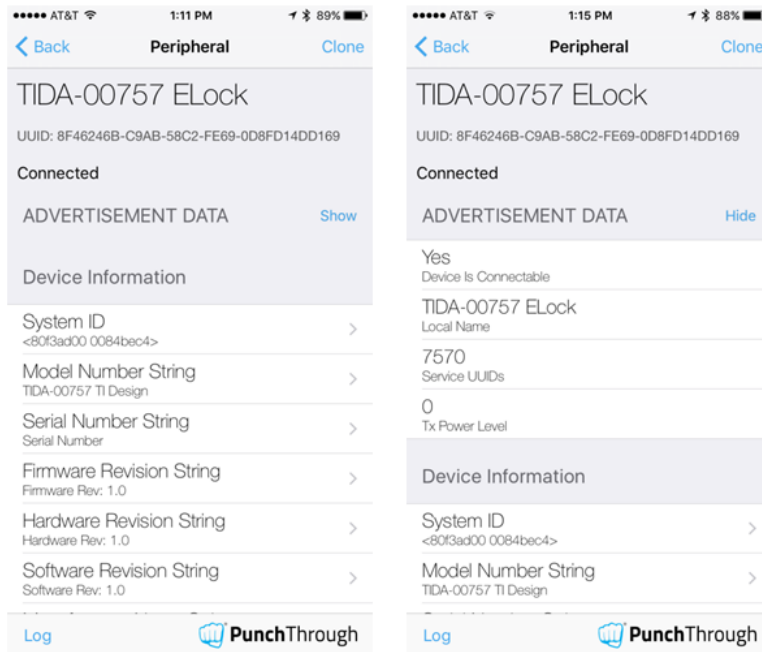


Figure 31. Advertisement Data Screen

10. Scroll to the bottom of the screen, and click on the *Lock State* attribute (see [Figure 32](#)).

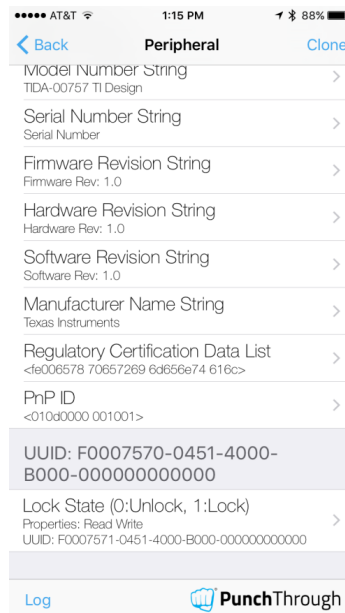


Figure 32. Lock State Screen

- After clicking the Lock State attribute, the device automatically reads the current lock state. In [Figure 33](#), the lock state is unlock (value 0). To change the value, click on the *Write new value* option. On the Android™ B-BLE app, the user must write two characters, either 00 or 01.

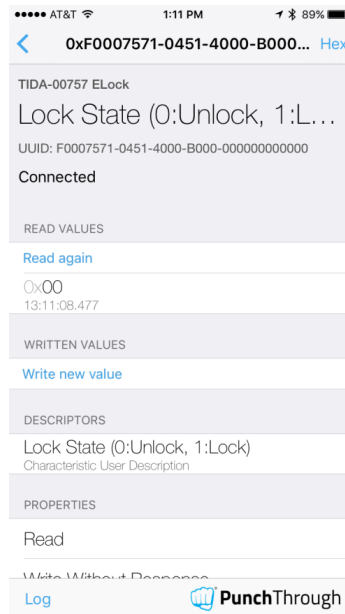


Figure 33. Lock State Values Screen

- Write the value 1 in the text box, and click done (see [Figure 34](#)). This triggers the attribute value change event, which turns the motor, and displays the LEDs accordingly.

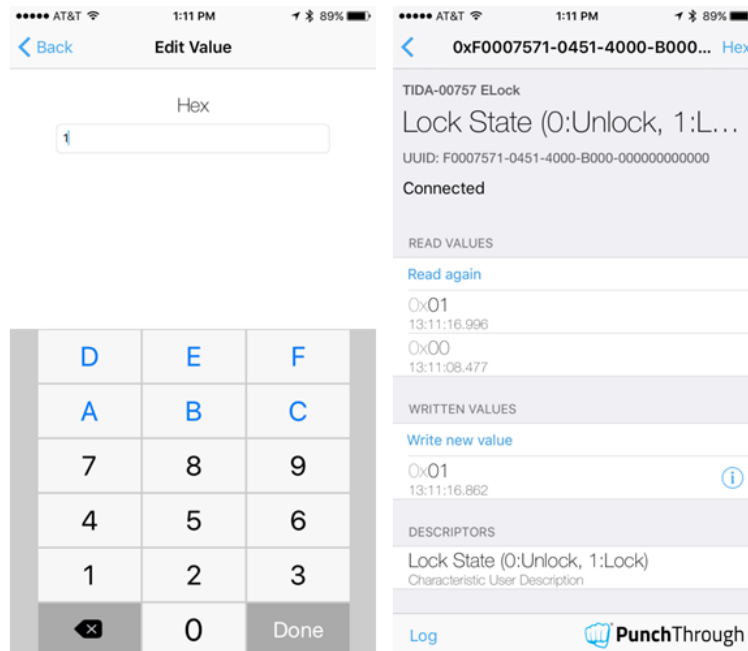


Figure 34. Selecting Lock State Value (1)

- Write the value 0 in the text box (see Figure 35), and click Done to spin the motor in the opposite direction.

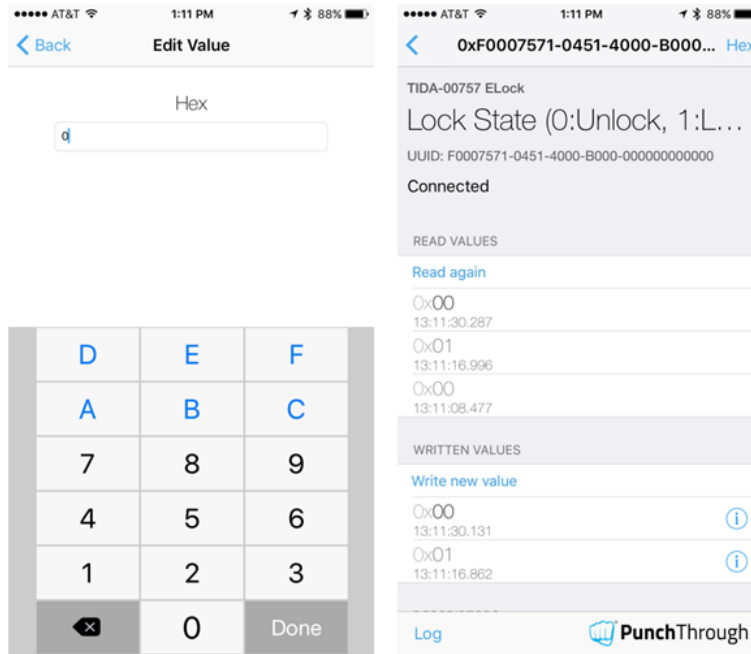


Figure 35. Selecting a Lock State Value (0)

- If a new value is not written within 30 seconds, the inactivity time-out event is triggered and disconnects the device (see Figure 36).

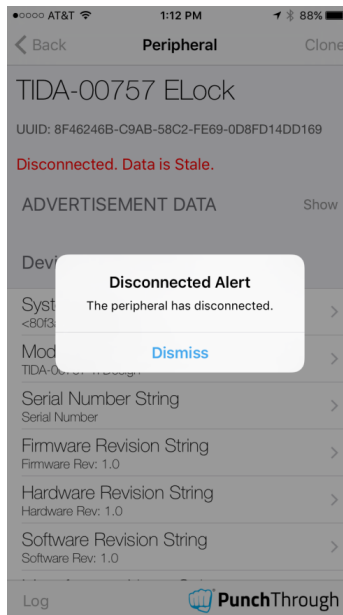


Figure 36. Inactivity Time-out Screen

7 Test Setup

Each of the different subsystems within the TIDA-00757 reference design were tested independently when possible to achieve a breakdown of power statistics which are summarized in [Section 8.5](#). This section of the document outlines how the tests were set up and conducted, if a user wants to recreate the results.

7.1 Power Supply

To standardize the results, the reference design is powered by a 5-V power supply because the batteries normally used to power the design can decrease in voltage over time. Five volts were chosen as the testing voltage because the batteries balance out at 5 V for the majority of the life of the batteries. Keep in mind that batteries have a current draw limit, whereas the power supply does not. Measurements were taken with batteries as a comparison because of the innate current limit of the batteries and are discussed as well. The power supply was connected to J1 and the ground test point, as shown in [Figure 37](#). [Figure 37](#) also shows the configuration of the current probe used to capture the higher current motor drive waveforms.

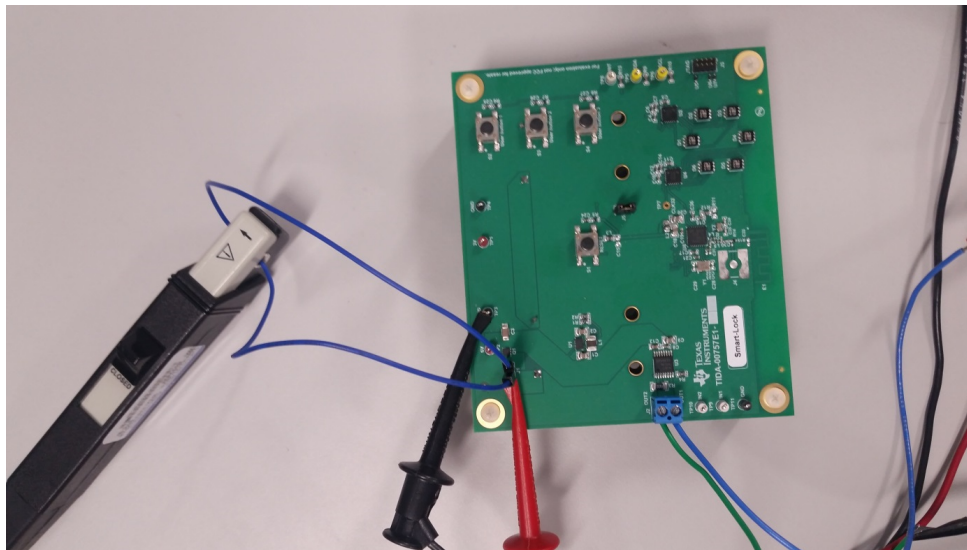


Figure 37. 5-V Power Supply Connection Configuration

7.2 Scope and Waveform Capture

A Tektronix® DPO 7054 Digital Phosphor Oscilloscope was used to capture the majority of the waveforms featured in this document. The Digital Phosphor Oscilloscope provides quick and easy capture of waveforms with averaging and peak values. The scope averages the points between horizontal markers to instantly give an accurate average, instead of just averaging the entire range on screen. The average calculated by the scope is implemented in the test results. A sense resistor was used when a current probe could not be used to measure the small amount of current for a specific test. The sense resistor is placed across the terminals of J1, as shown in [Figure 38](#). A multimeter was used to accurately measure the resistance of the sense resistor before putting the resistor into the circuit.

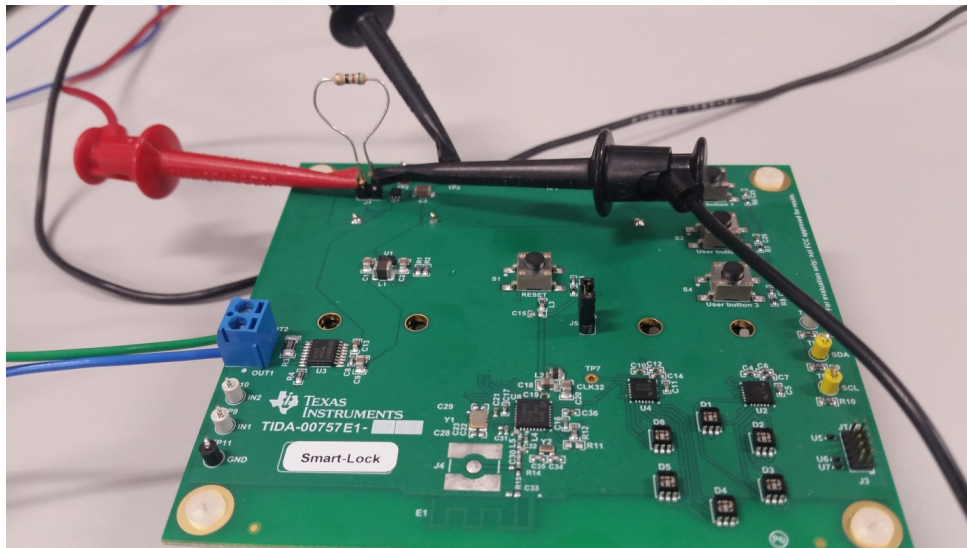


Figure 38. Sense Resistor Test Configuration on J1

7.3 Motor Loading

To accurately simulate normal operating conditions of a motorized door lock, the motor is connected to a standard deadbolt assembly, which is installed onto a normal door. The motor is connected to the deadbolt cylinder by taking the place of the thumb turn assembly. The motor is connected with a simple keyed shaft collar which allows a small amount of slop. The slop allows the motor to start spinning before the torque from the deadbolt is applied to the motor. This design lets the motor use a little less current to get it to start turning.

The deadbolt has 1 inch of throw and the motor must run for approximately 1.8 seconds to lock or unlock the bolt. All testing and measurements are completed using 1.8 seconds as the motor run time for loaded and unloaded motor tests. The DC mini-motor is rated for 4 V with a rated load of 9.3 mN-m.

8 Test Data

NOTE: Unless otherwise noted, the test data in the following sections was measured with the system at room temperature. All of the measurements in this section were measured with calibrated lab equipment.

8.1 Power System Tests

8.1.1 Buck Output and Efficiency

The input voltage at J1 varied from 6.4 V to 3.7 V, and the voltage on the 3-V rail was measured at TP1 and TP2. [Table 3](#) lists the results.

Table 3. Input Voltage Versus Buck Output

INPUT VOLTAGE (V)	BUCK OUTPUT (V)
6.4	3.00
6.0	3.00
5.6	3.00
5.2	3.00
5.0 (nominal)	3.00
4.8	3.00
4.4	3.00
4.0	3.00
3.7	3.00

The efficiency of the TPS62745 was simulated with TI's WEBENCH® Design Tool. The graphs in [Figure 39](#) and [Figure 40](#) show the results.

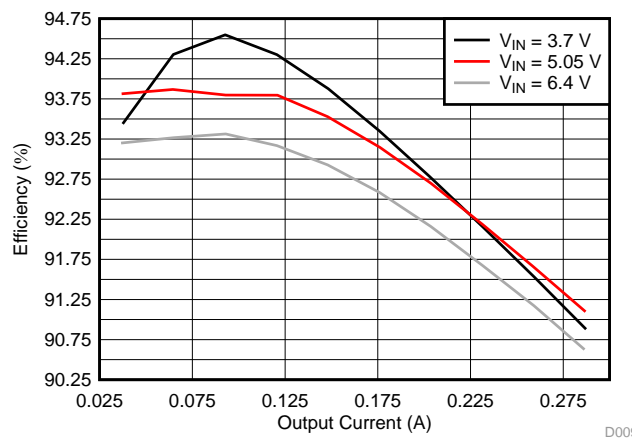


Figure 39. Buck Output Current Versus Efficiency (TPS62745)

Figure 40 shows a wider current range of the efficiency results.

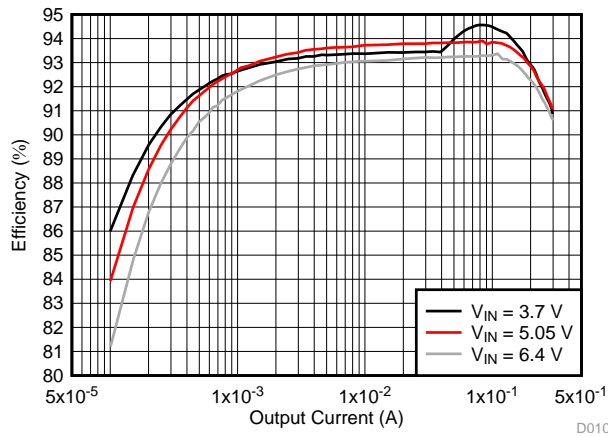


Figure 40. Buck Output Current Versus Efficiency, Wider Current Range (TPS62745)

8.1.2 Input Voltage Versus Average Current Consumption

The batteries decrease in voltage over time, but settle at a nominal voltage of 5 V. The majority of the testing done on the TIDA-00757 reference design is completed at the nominal voltage of 5 V with a power supply. However, batteries have innate current limiting, and the results may vary slightly depending on which batteries are used and how old they are, whereas the power supply has no current limit. Table 4 captures and records the peak current and average current for the motor operation state. The range of 6.4 V to 3.7 V was chosen because the maximum voltage of four AA batteries can be close to 6.4 V and the minimum V_{in} of the buck is 3.7 V.

Table 4. Input Voltage Versus Average Current

INPUT VOLTAGE	PEAK CURRENT (A)	AVG CURRENT (mA)	BUCK OUTPUT (V)
6.4	2.46	45.20	3.0
6.0	2.38	45.09	3.0
5.6	2.32	45.05	3.0
5.2	2.17	45.86	3.0
5.0 (nominal)	2.099	49.52	3.0
4.8	2.007	53.10	3.0
4.4	1.848	55.63	3.0
4.0	1.68	58.96	3.0
3.7	1.54	60.24	3.0

8.2 Bluetooth® low energy Communications

The Bluetooth low-energy tests included looking at the advertisement packet timing and current consumption waveforms, along with examining the connected packet timing and current waveforms. A sense resistor was used to measure the small amount of current in the system during the Bluetooth connection periods. Section 7 describes the sense resistor method.

Figure 41 shows the equivalent current waveform. The voltage readings were averaged over the time of the packet pulse time and a 50.048-Ω sense resistor was used.

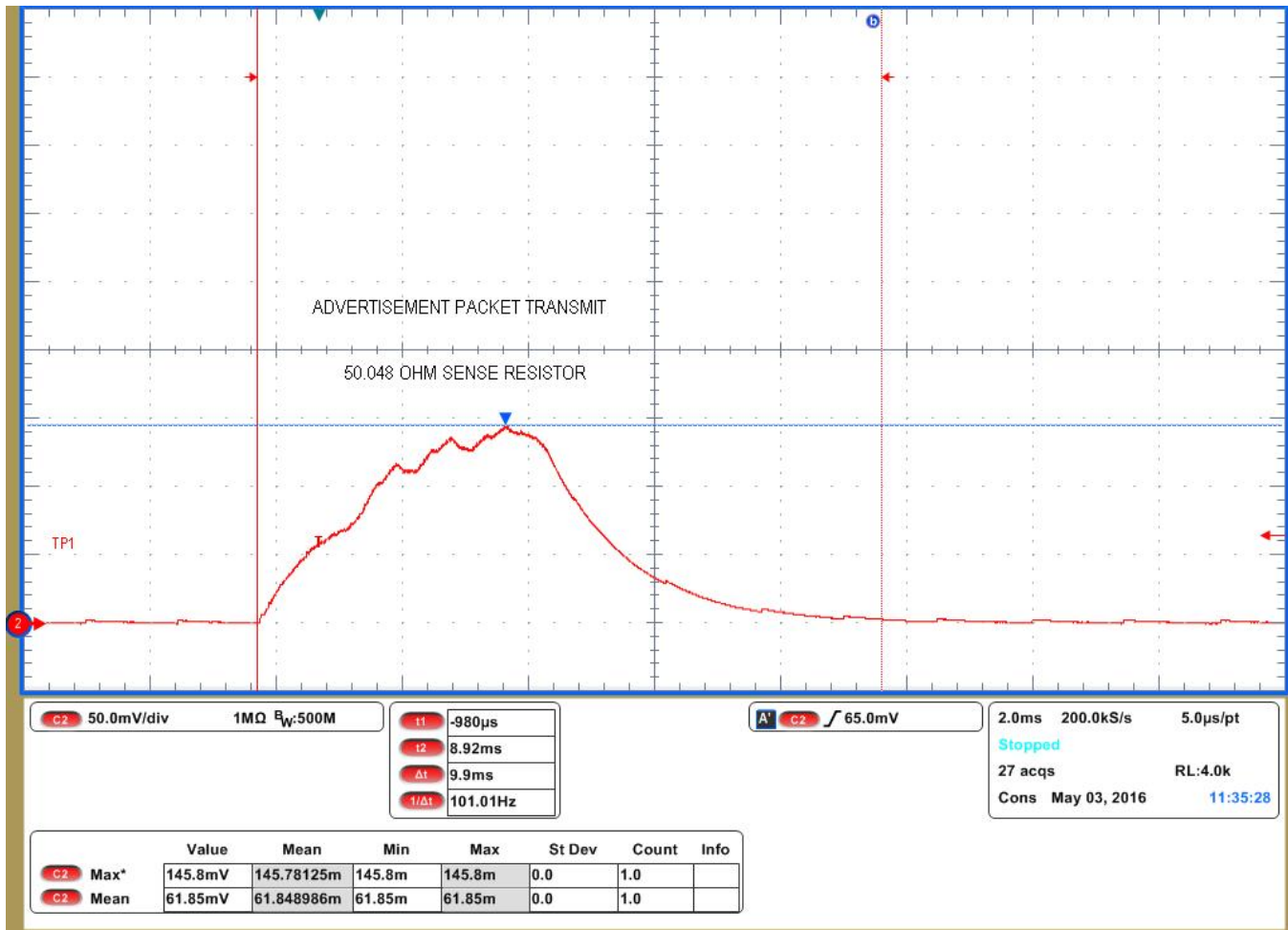


Figure 41. Bluetooth® low energy Advertisement Packet

The average voltage is 61.849 mV, so dividing voltage by resistance allows us to solve for average current. The average current is 1.236 mA over the pulse width of approximately 9.9 ms.

$$\text{average current} = (61.849 \text{ mV}) / (50.048 \ \Omega) = 1.236 \text{ mA} \tag{14}$$

Figure 42 shows the advertisement packet transmit period. The TIDA-00757 reference design broadcasts its basic information and advertises its presence to allow devices to connect to it every 500 ms. Figure 42 is the zoomed out view of the advertisement pulses seen in Figure 41. The tiny pulses seen between the transmits are the internal DC/DC converter of the CC2640R2F charging up for the next transmission.

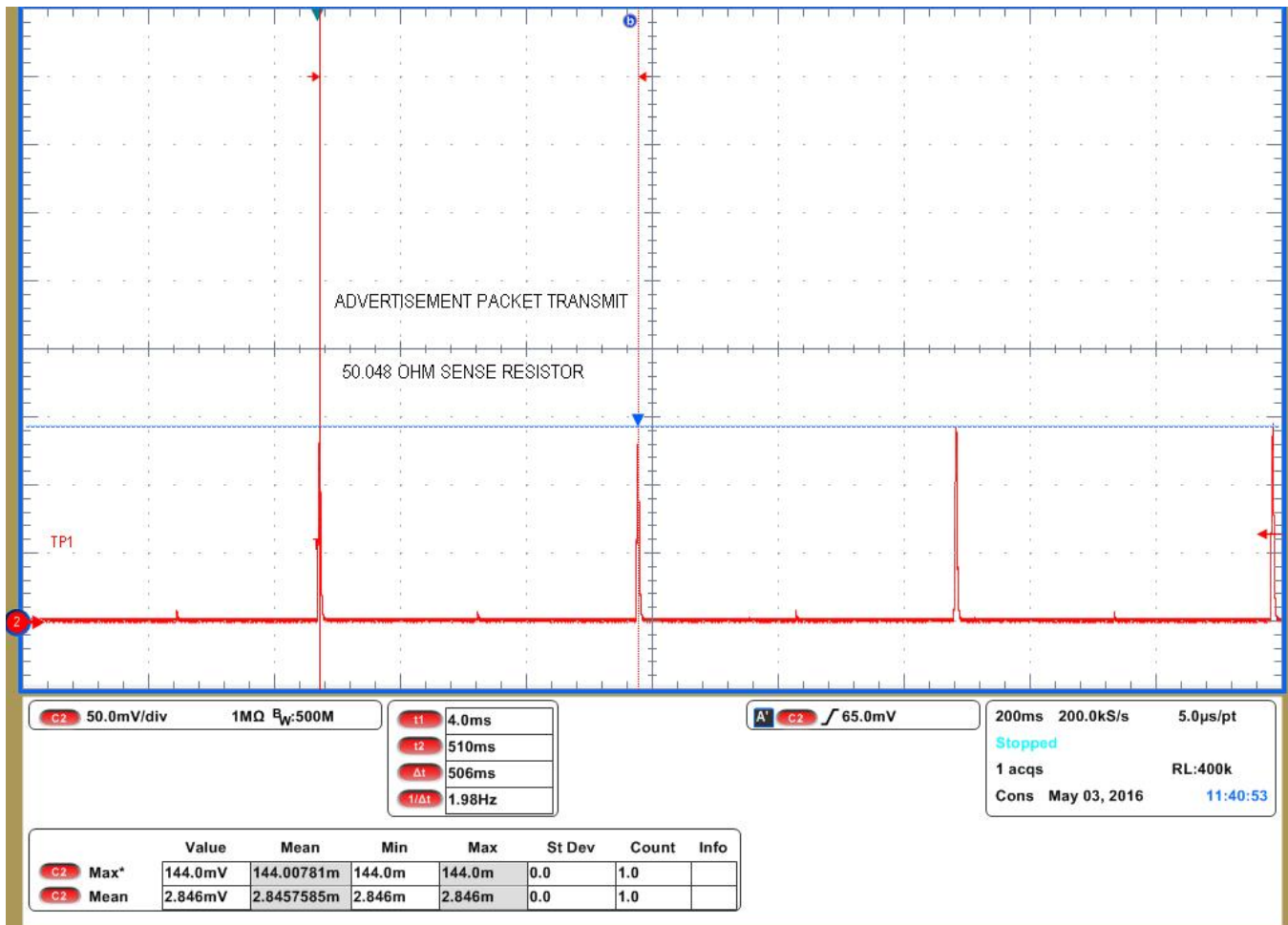


Figure 42. Bluetooth® low energy Advertisement Transmit Period

Once a device is paired with the TIDA-00757 reference design the current consumption of the design looks slightly different. Figure 43 shows what the waveform of each connected pulse looks like. The maximum voltage is slightly lower and the pulse length is shorter.

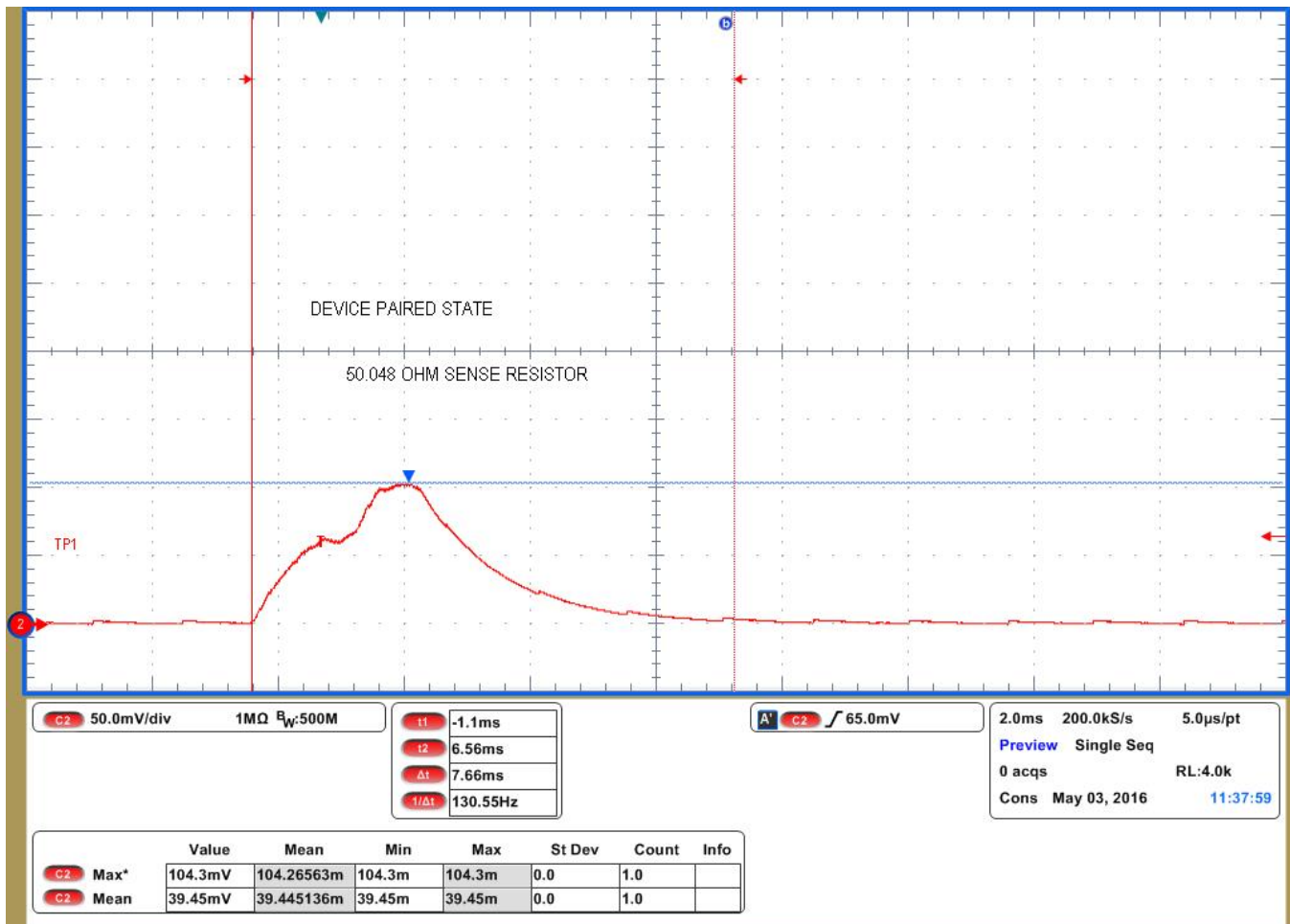


Figure 43. Bluetooth® low energy Device Paired Packet

Equation 15 describes how to calculate the average current for the connected pulse.

$$\text{avg current} = (39.445 \text{ mV}) / (50.048 \Omega) = 0.788 \text{ mA} \quad (15)$$

The average current for a single connected pulse lasting approximately 7.66 ms = 0.788 mA.

Once a device is connected to the TIDA-00757 reference design, the average current pulse becomes slightly smaller. However, the pulse period is shortened to decrease latency in the user experience.

As seen in Figure 44, the period is 30 ms when a device is connected. The 30 ms transmit period stays in effect for 30 seconds after the last input from the user's device. More discussion of the software algorithm is discussed in Section 3.7.

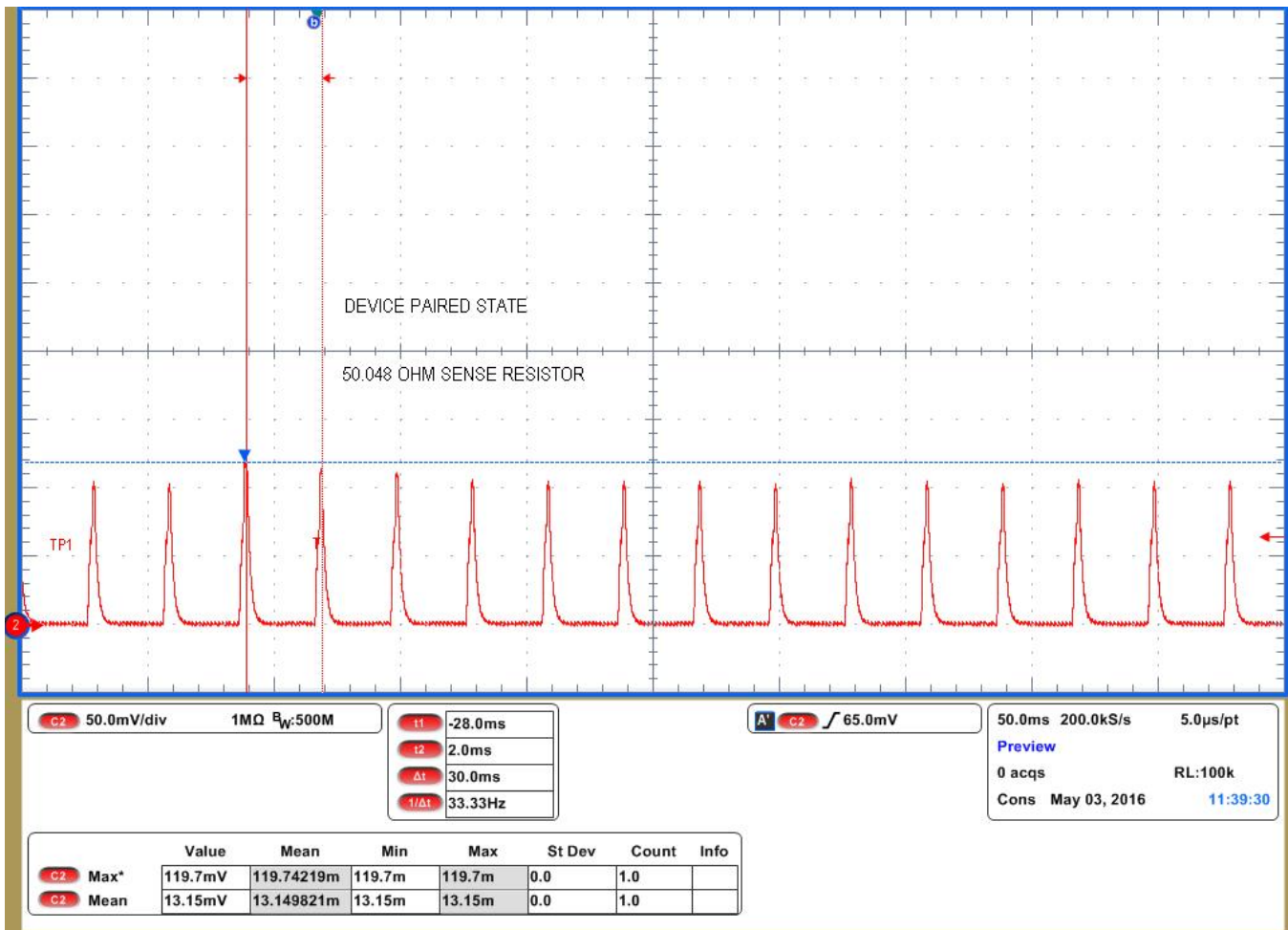


Figure 44. Bluetooth® low energy Device Paired Packet Transmit Period

8.3 Standby Current

The average standby current can be found by measuring the current consumption between advertisement packet transmissions. During this time the other devices in the TIDA-00757 reference design are in standby or sleep mode, allowing an accurate measurement of the standby current. A small sense resistor was used to measure the small amount of current. The average standby current of this reference design with the algorithm discussed in Section 3.7 is approximately 4.7 μ A.

8.4 Motor Current

This section covers each of the different motor current waveforms for a loaded and unloaded motor, with LEDs on and off. Unloaded means the motor was free spinning and loaded means the motor was connected to the deadbolt, and a successful lock or unlock occurred. Each lock or unlock event takes 2 seconds total. The motor only stays on for 1.8 seconds, but the LED pattern sequence is 2 seconds long. All average calculations are calculated over a 2 second time interval.

8.4.1 Unloaded Motor Current Waveforms

Batteries have innate current limiting and because of this feature the maximum current spike when the motor started spinning is 1.259 A, with an average current of 27.67 mA over the 2 second unlock event. Figure 45 shows the battery powered unloaded unlock event waveform.

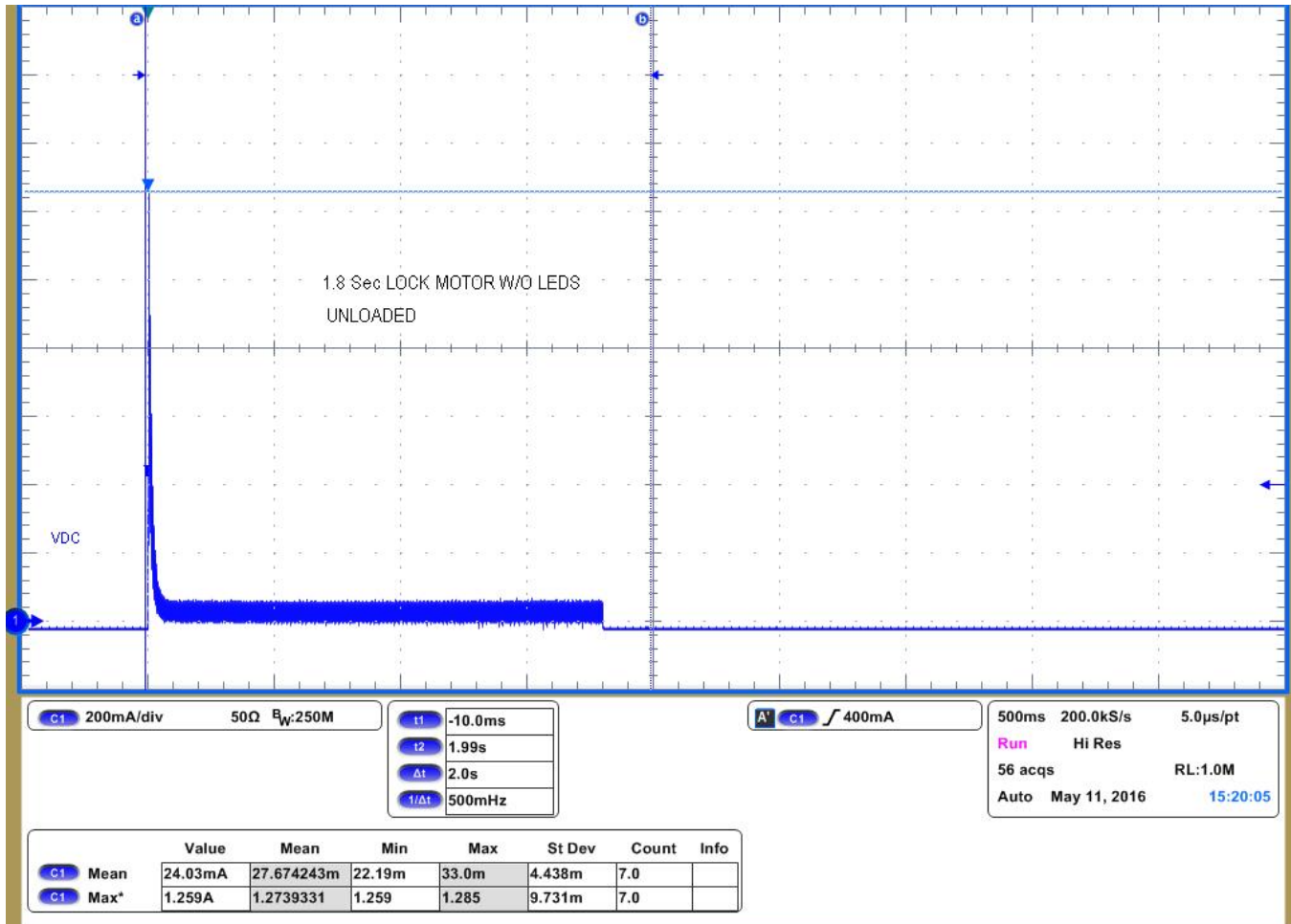


Figure 45. 1.8 Second Unloaded Motor Unlock Without LEDs Enabled on Four AA Batteries

Figure 46 shows the same unloaded unlock event, but the reference design is being powered by the 5 V power supply. The starting current spike is much larger because the power supply is not limiting the current. On batteries the current spike is 1.259 A, whereas the power supply current spike is 1.92 A. The increased spike greatly increases the average current from 27.67 mA to 43.717 mA.

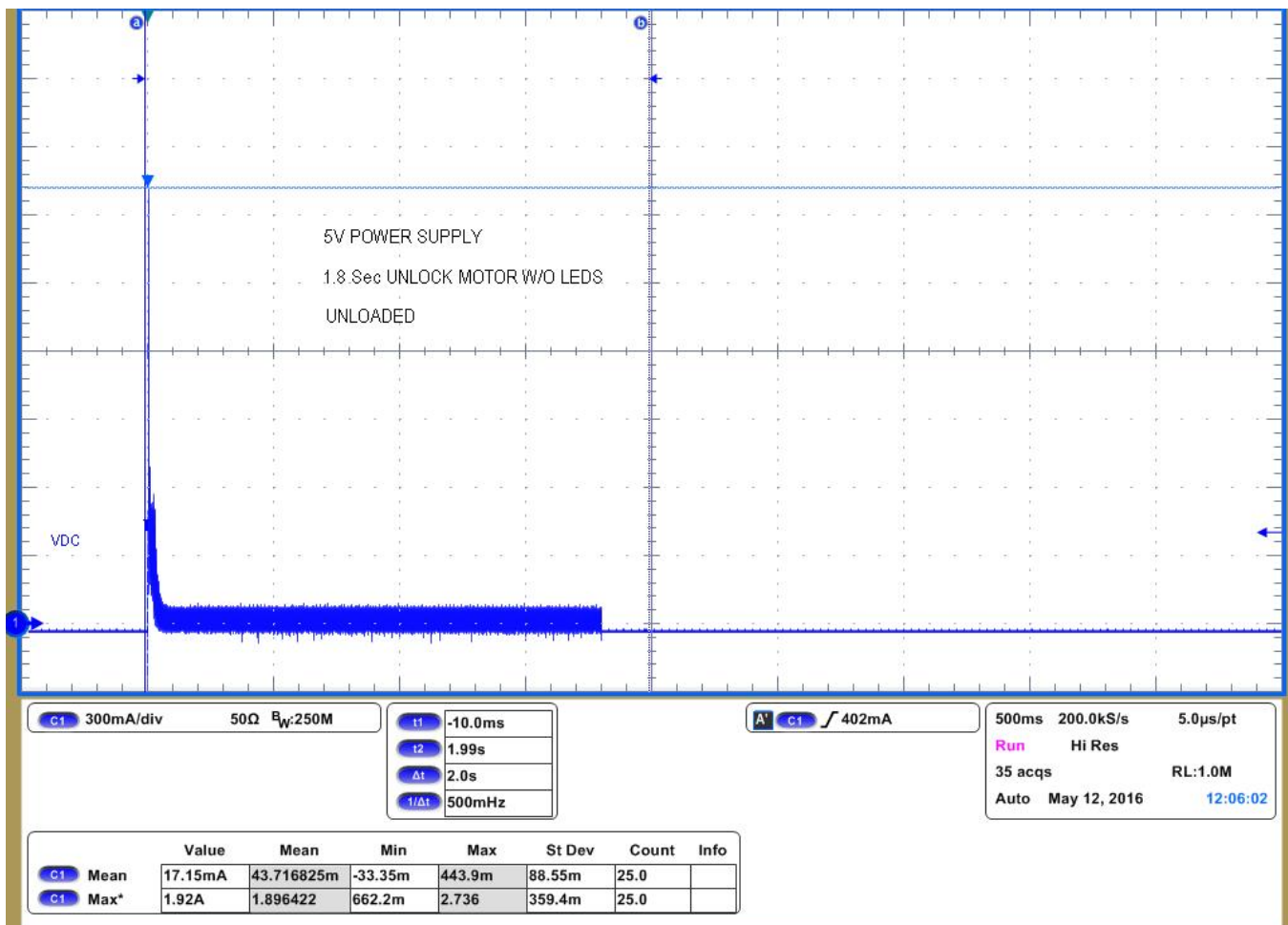


Figure 46. 1.8 Second Unloaded Motor Unlock Without LEDs Enabled

From now on, only the waveforms captured while the reference design is powered by the power supply are used to calculate the current consumption to standardize the results. Five volts was chosen as the testing voltage because the batteries balance out at 5 V for the majority of the life of the batteries. One thing to remember is that batteries have a current draw limit, whereas the power supply does not.

Figure 47 shows the unloaded lock event with the LEDs disabled. The lock event average current is slightly different than the unlock event. The average current is 42.756 mA over 2 seconds. This result could be because the current spike at the beginning is slightly smaller and the rest of the waveform is a little smoother.

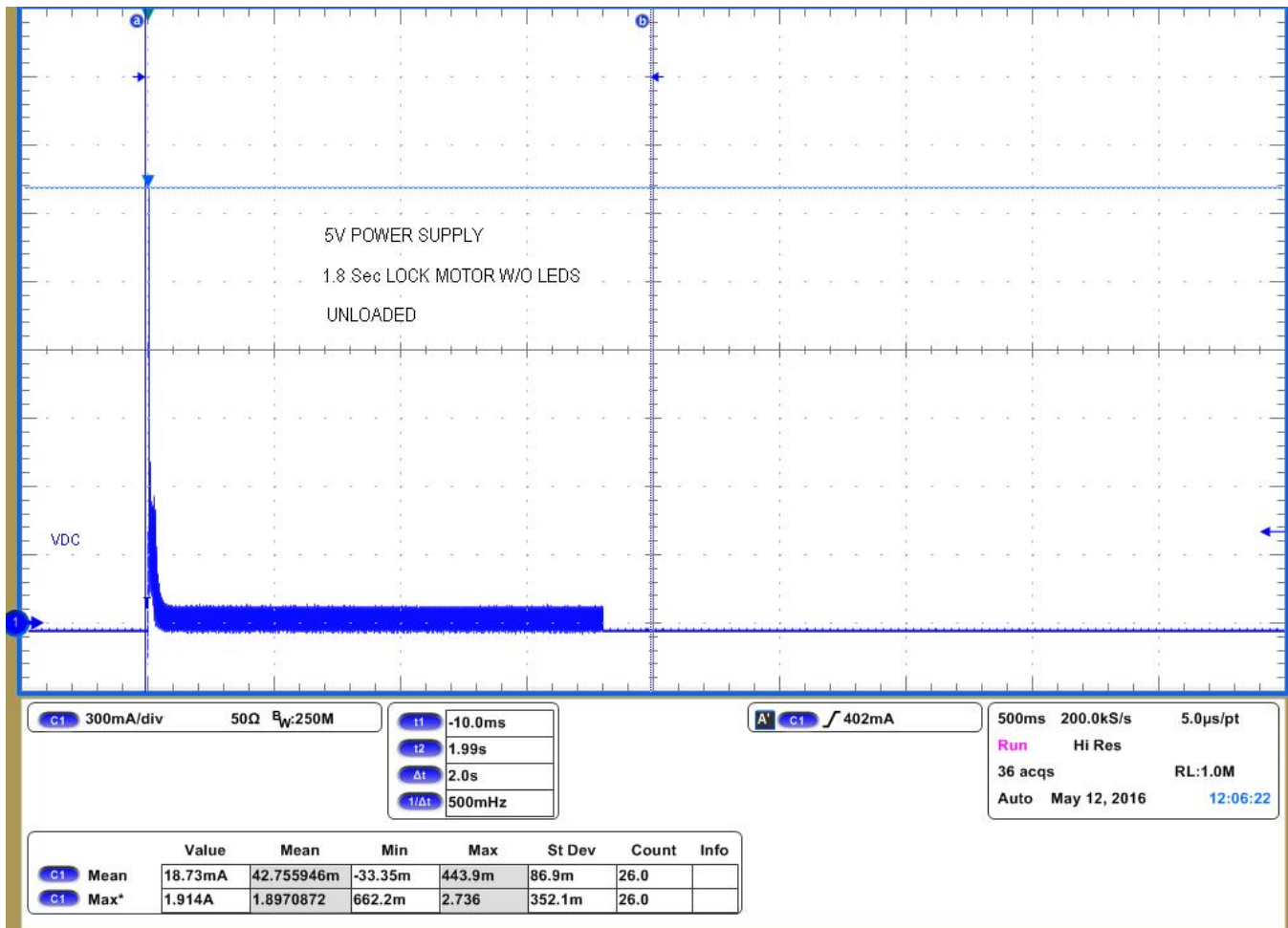


Figure 47. 1.8 Second Unloaded Motor Lock Without LEDs Enabled

Figure 48 shows the unloaded lock event with the LEDs enabled. The average is slightly lower even though the LEDs are also on. The current spike is also lower than the previous waveforms which better explains why the average is lower.

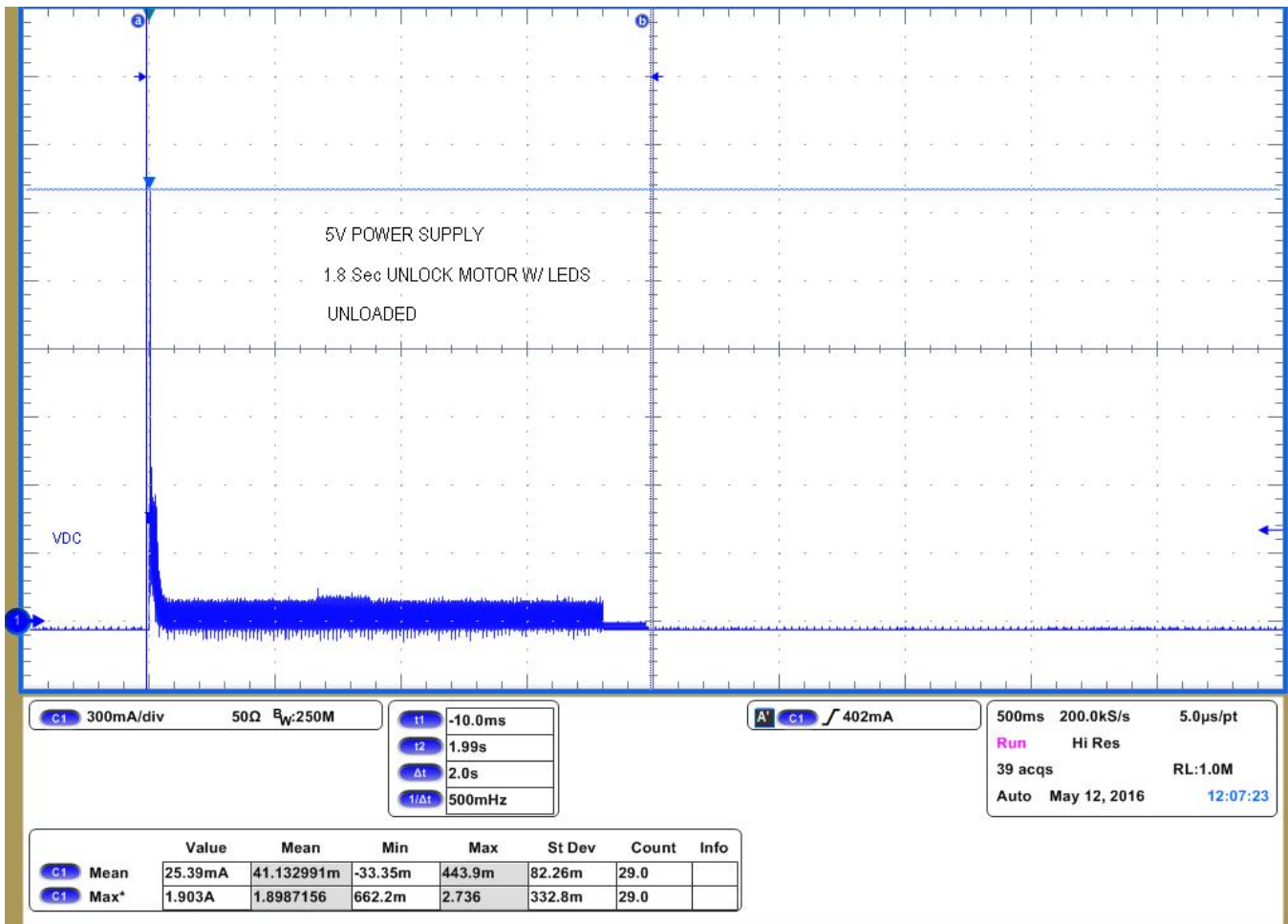


Figure 48. 1.8 Second Unloaded Motor Unlock With LEDs Enabled

The LED sequence lasts for the full 2 seconds. The end of the LED sequence can be seen in the scope capture, look at the last 0.2 seconds after the motor waveform has finished and the LED current can be seen. Figure 49 shows the end of LED sequence.

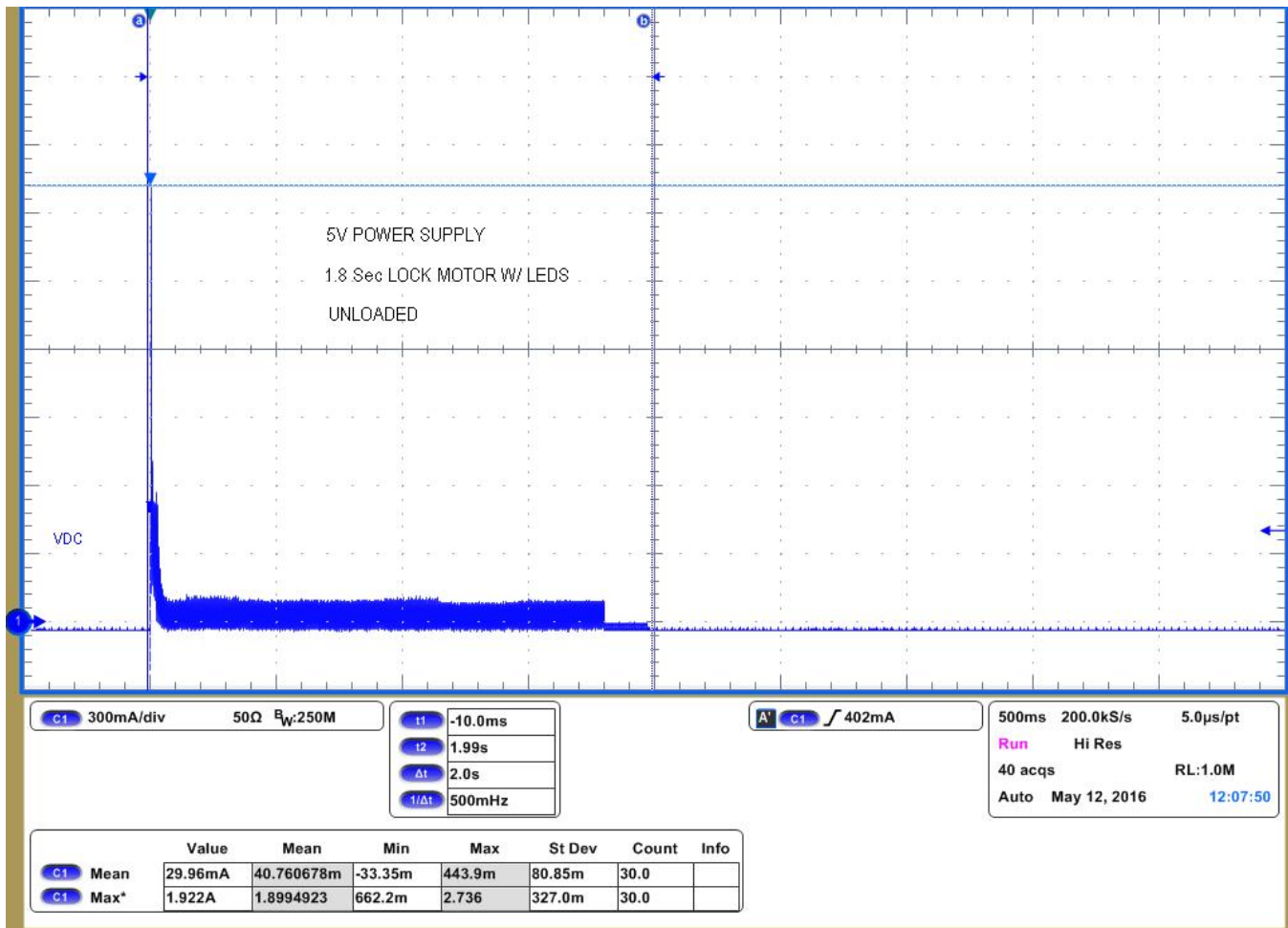


Figure 49. 1.8 Second Unloaded Motor Lock With LEDs Enabled

8.4.2 Unloaded Motor Current Summary

Table 5 summarizes all the results of the unloaded testing. The 5 V power supply was used to standardize, instead of using batteries which give varying results because of battery drain.

Table 5. Unloaded Motor Results Summary

UNLOADED MOTOR CONFIG (5 V)	PEAK CURRENT	AVERAGE CURRENT
Unlock (no LEDs)	1.920 A	43.717 mA
Lock (no LEDs)	1.914 A	42.776 mA
Unlock (with LEDs)	1.903 A	41.132 mA
Lock (with LEDs)	1.922 A	40.761 mA

8.4.3 Loaded Motor Current Waveforms

The DC motor consumes a little more current when it is under load, which is to be expected. This section contains the current waveform captures and averages for door lock and unlock actions while the motor is actually connected to the deadbolt assembly. For an explanation of how the motor is connected to the deadbolt, refer to [Section 7.3](#) in [Section 7](#) of this document. [Figure 50](#) shows the first waveform capture of the deadbolt unlock action without LEDs. The current spike at the beginning is the same as seen on an unloaded motor. The end portion of the waveform is different because the current starts to ramp up slightly as the deadbolt starts loading the motor and also at the very end when the deadbolt has reached the length of its extension.

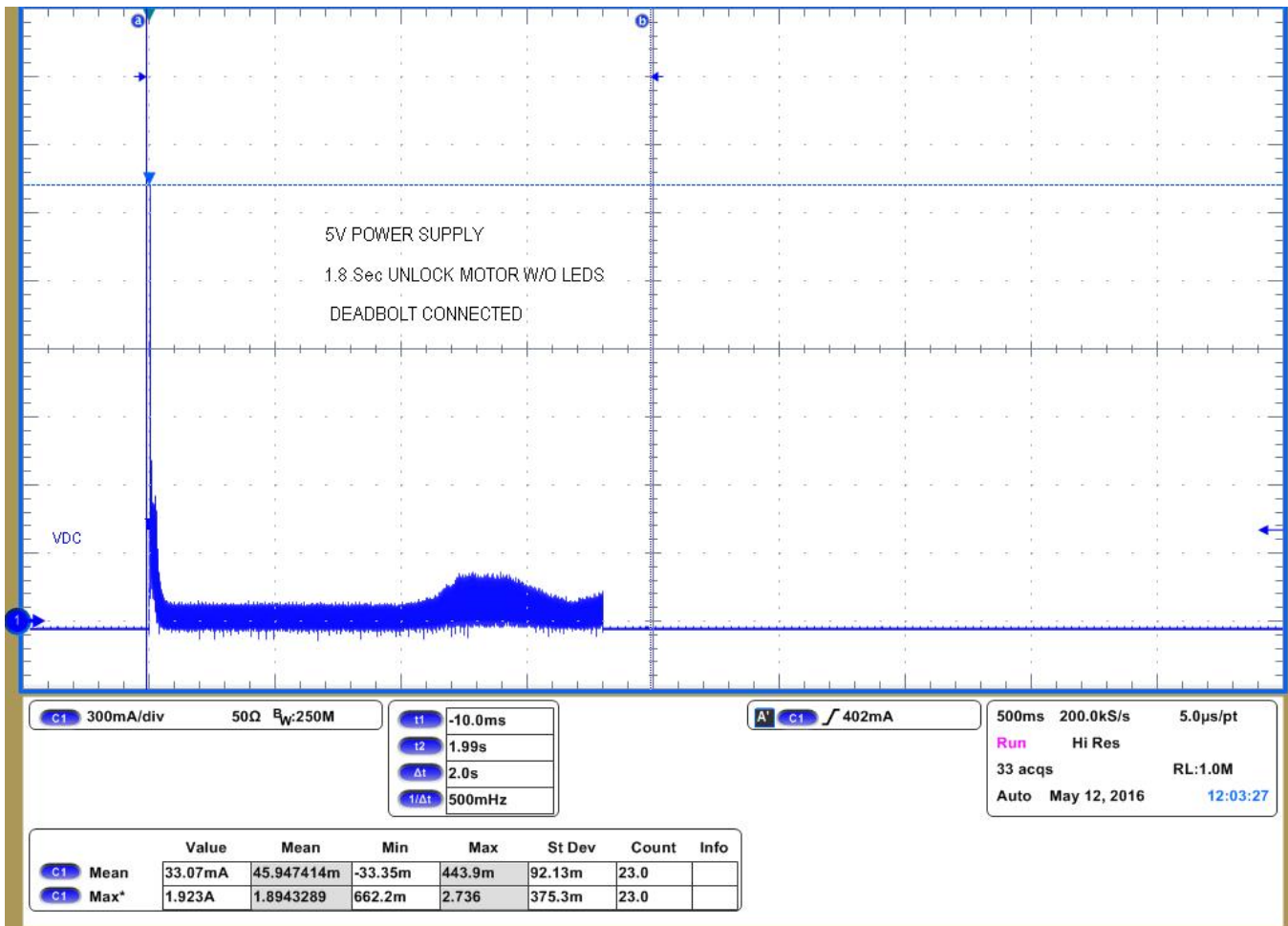


Figure 50. 1.8 Second Loaded Motor Unlock Without LEDs Enabled

Locking the deadbolt without LEDs active has a very similar current waveform, shown in Figure 51. The average current for unlocking the deadbolt without LEDs is approximately 46 mA for 2 seconds. The average current for locking is approximately 48 mA for 2 seconds.

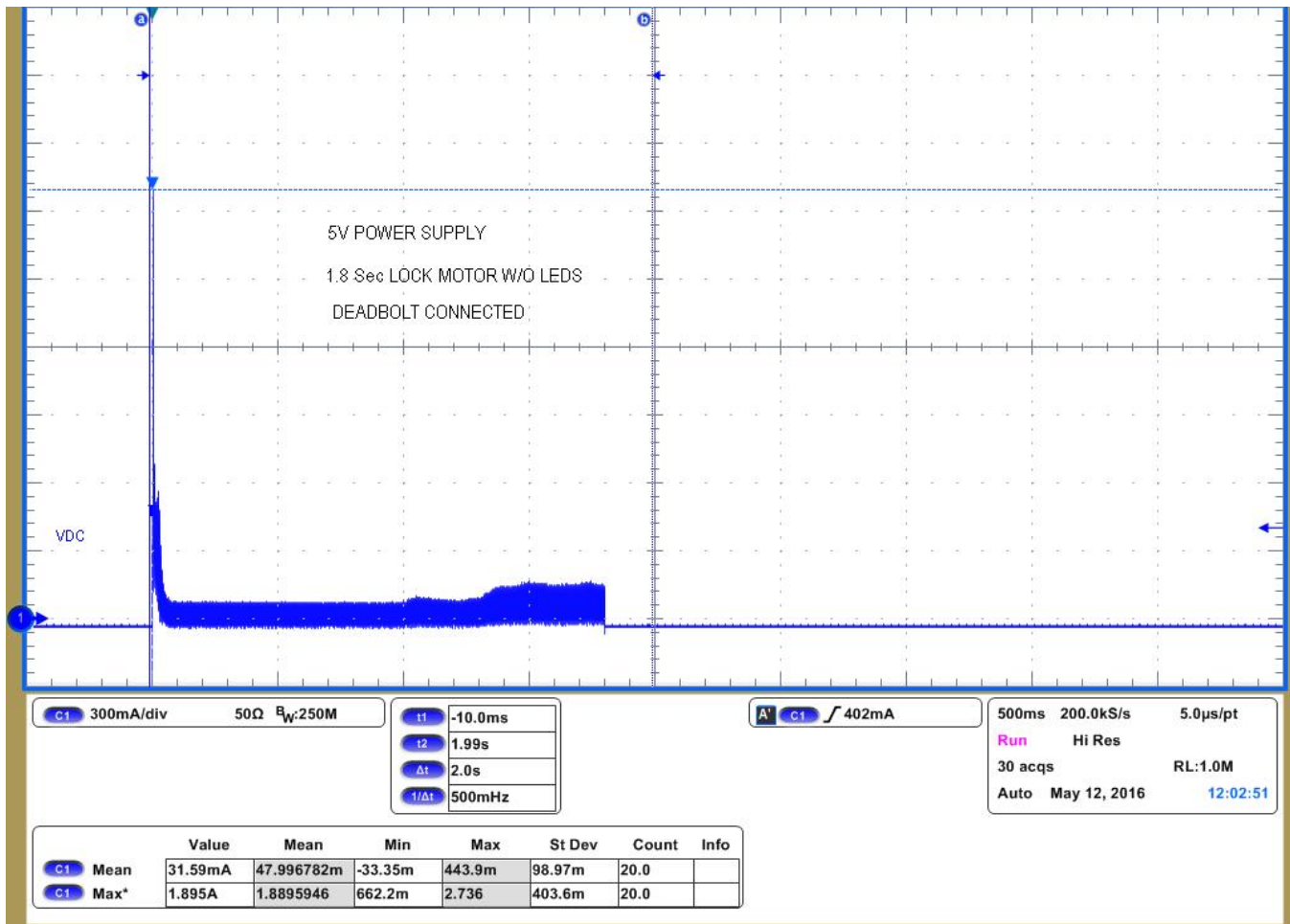


Figure 51. 1.8 Second Loaded Motor Lock Without LEDs Enabled

When the LEDs are enabled it adds about 2 mA to the average current consumption over the 2 second unlocking or locking event. Figure 52 and Figure 53 show the unlock and lock event waveforms, respectively. The average current consumption for unlocking is 48 mA and the lock average current is 50 mA.

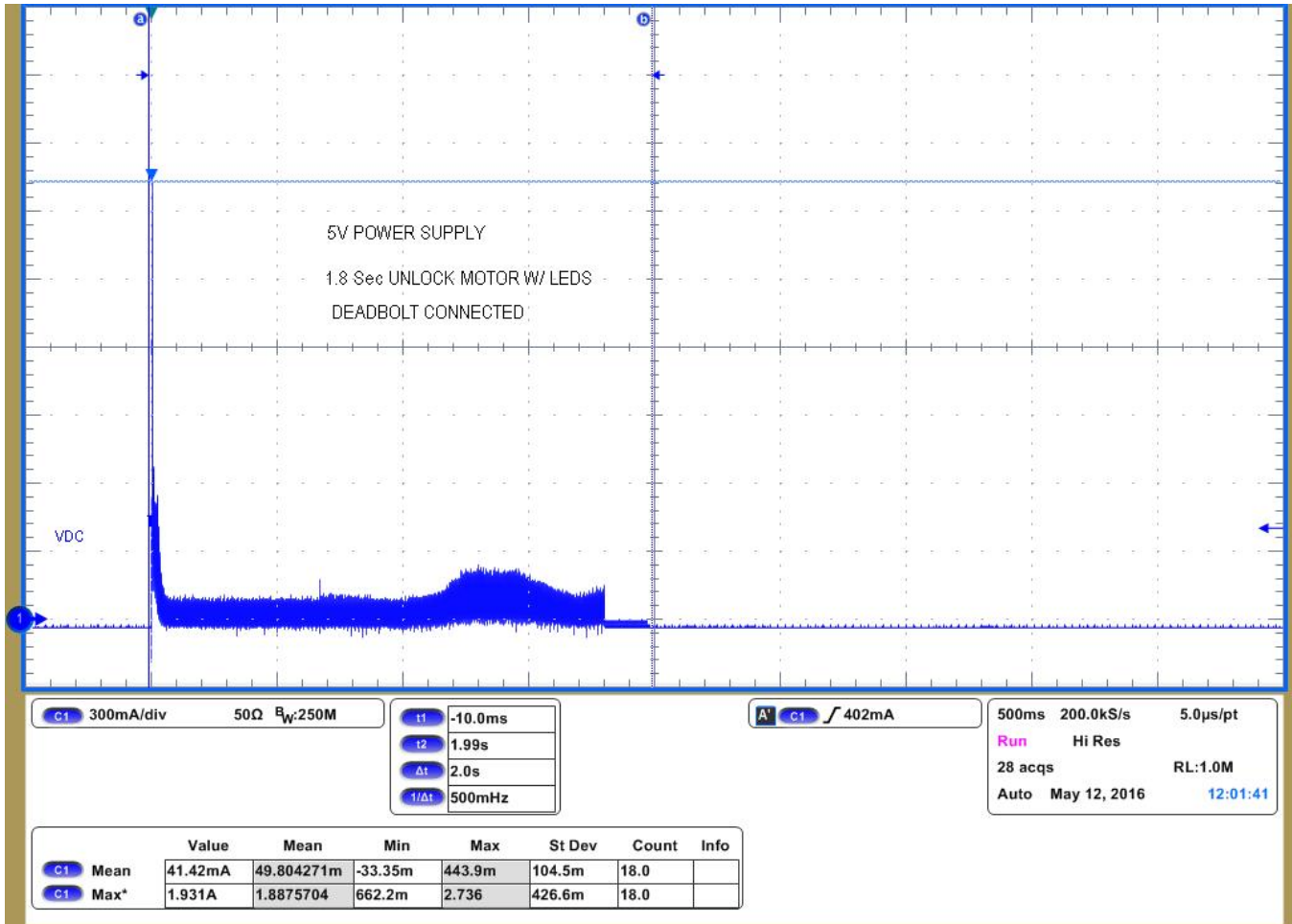


Figure 52. 1.8 Second Loaded Motor Unlock With LEDs Enabled

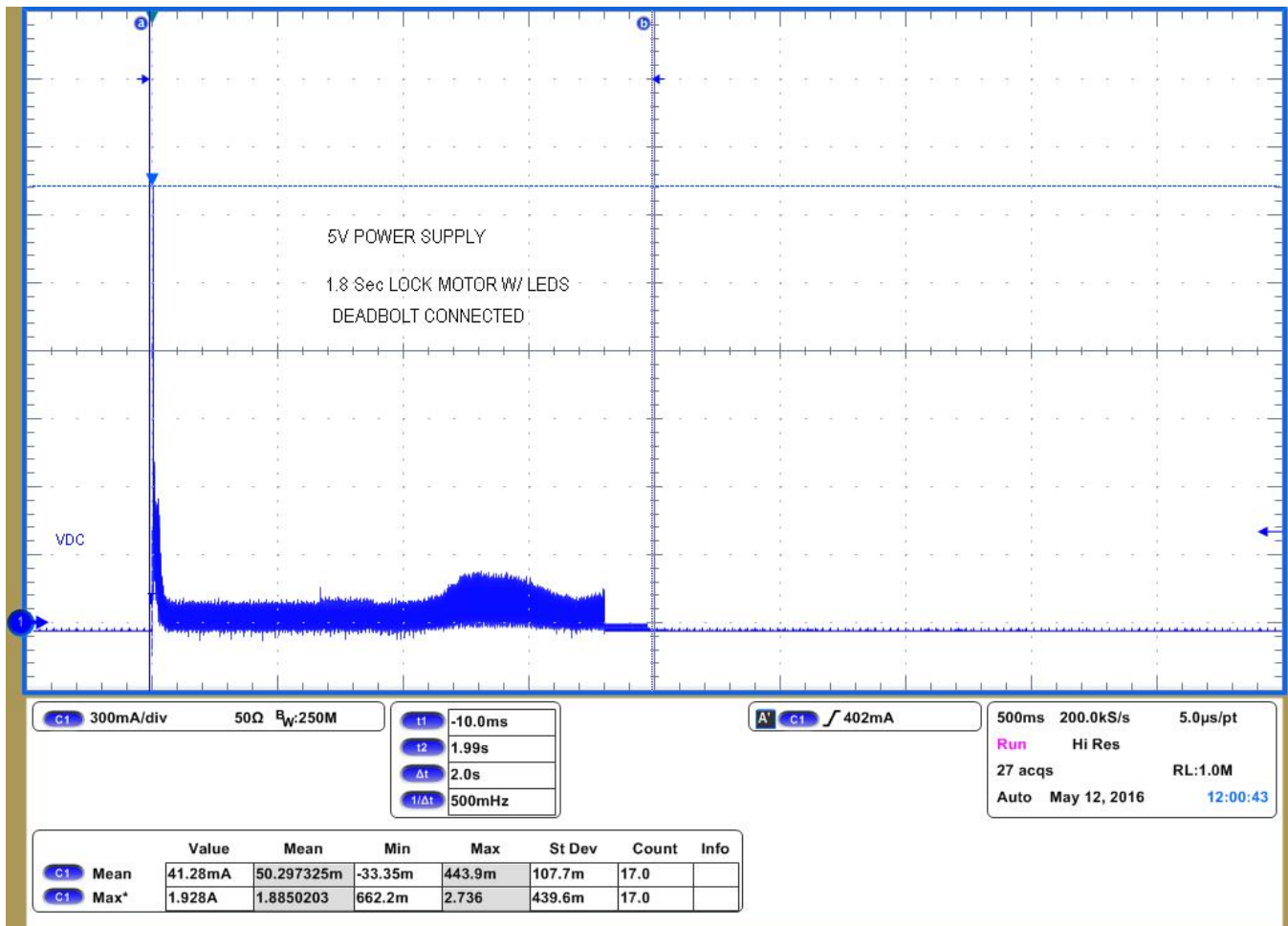


Figure 53. 1.8 Second Loaded Motor Lock With LEDs Enabled

8.4.4 Loaded Motor Summary

Table 6 summarizes all the results of the motor connected to the deadbolt. The 5-V power supply was used to standardize results, instead of using batteries which would give varying results because of battery drain.

Table 6. Unloaded Motor Results Summary

LOADED MOTOR CONFIG (5V)	PEAK CURRENT	AVERAGE CURRENT
Unlock (no LEDs)	1.923 A	45.947 mA
Lock (no LEDs)	1.895 A	47.997 mA
Unlock (with LEDs)	1.931 A	49.804 mA
Lock (with LEDs)	1.928 A	50.297 mA

8.5 Estimated Battery Life

To easily calculate the estimated battery life, each of the TIDA-00757 reference design states has been separated. The average current for: standby, Bluetooth low energy advertisement, Bluetooth low energy connected, and motor and LED operation states have been gathered during testing. The average current per event, time per event, and total time in that state must be calculated or measured to estimate how much current is consumed in each state. A 24-hour time frame is used for the calculations because 24 lock or unlock events are being assumed in a 24 hour period. A 24 hour period also makes calculating battery life in years easier to convert.

NOTE: Unless otherwise noted, the battery capacity calculations in the following sections are done in mAh and not mW-h.

8.5.1 Motor and LED Average Current

The average current for the motor and LEDs was measured in [Section 8.4](#). The highest current-consumption measurement is considered for these current calculations. An average current of 50 mA for 2 seconds was measured during the lock event with the LEDs operating. To find the average current consumption over a 24 hour period use [Equation 16](#) and [Equation 17](#).

$$\text{Duty Cycle of Motor State} = \text{Events} \times \text{Event Duration} \times \frac{1}{24 \text{ hrs}} \times \frac{1}{60 \text{ mins}} \times \frac{1}{60 \text{ secs}} \quad (16)$$

$$\text{Motor } I_{\text{avg}} = \text{LED and Motor } I_{\text{avg}} \times \text{Events} \times \text{Event Duration} \times \frac{1}{24 \text{ hrs}} \times \frac{1}{60 \text{ mins}} \times \frac{1}{60 \text{ secs}} \quad (17)$$

$$\text{Motor } I_{\text{Avg}} = 50 \text{ mA} \times 24 \times 2 \text{ secs} \times \frac{1}{24 \text{ hrs}} \times \frac{1}{60 \text{ mins}} \times \frac{1}{60 \text{ secs}} \quad (18)$$

$$\text{Motor } I_{\text{Avg}} = 0.028 \text{ mA}$$

8.5.2 Bluetooth® low energy Connected State Average Current

Because the average current for a single Bluetooth low energy connected pulse was measured, the total current consumption for 24 hour period can be calculated. The average current is 0.788 mA for 7.6 ms. The number of Bluetooth low energy connected pulses in the 30-second connected time must be calculated. The LED and motor current measurement included the connected pulses, so the motor event lasting 2 seconds must be subtracted from the connected period. The connection period is the time between pulses, or 30 ms.

$$\text{BLE Connected Pulses Per Event} = \frac{\text{Connected Time} - \text{Motor Event Time}}{\text{Connection Period}} \quad (19)$$

$$\text{BLE Connected Pulses Per Event} = \frac{30 \text{ sec} - 2 \text{ sec}}{0.03 \text{ sec}} \quad (20)$$

$$\text{Duty Cycle of Connected State} = \text{BLE Connected Pulses} \times \text{Events} \times \text{Event Duration} \times \frac{1}{24 \text{ hrs}} \times \frac{1}{60 \text{ mins}} \times \frac{1}{60 \text{ secs}} \quad (21)$$

$$\text{Connected } I_{\text{avg}} = \text{Connected } I_{\text{avg}} \times \text{BLE Connected Pulses} \times \text{Events} \times \text{Event Duration} \times \frac{1}{24 \text{ hrs}} \times \frac{1}{60 \text{ mins}} \times \frac{1}{60 \text{ secs}} \quad (22)$$

$$\text{Connected } I_{\text{avg}} = 0.788 \text{ mA} \times \frac{30 - 2}{.03 \text{ sec}} \times 24 \times .0076 \text{ sec} \times \frac{1}{24 \text{ hrs}} \times \frac{1}{60 \text{ mins}} \times \frac{1}{60 \text{ secs}} \quad (23)$$

$$\text{Connected } I_{\text{avg}} = 0.001553 \text{ mA}$$

8.5.3 Bluetooth® low energy Advertisement State Average Current

The average current during the Bluetooth low energy advertisement pulse is 1.235 mA over 9.9 ms. The CC2640R2F is sending advertisement packets only when it is not connected to a device, or when the motor is running, therefore these periods must be subtracted from the run time of the Bluetooth low energy advertisement state.

$$\text{Number of BLE Advertisement Packets} = \frac{24 \text{ hrs} \times 60 \text{ mins} \times 60 \text{ secs} - (\text{Connected Time} \times \text{Events})}{\text{Advertising Period}} \quad (24)$$

$$\text{Duty Cycle of Advertisement State} = \text{BLE Advertisement Pulses} \times \text{Pulse Duration} \times \frac{1}{24 \text{ hrs}} \times \frac{1}{60 \text{ mins}} \times \frac{1}{60 \text{ secs}} \quad (25)$$

$$\text{Advertisement } I_{\text{avg}} = \text{Advertisement } I_{\text{avg}} \times \text{BLE Advertisement Pulses} \times \text{Events} \times \text{Event Duration} \times \frac{1}{24 \text{ hrs}} \times \frac{1}{60 \text{ mins}} \times \frac{1}{60 \text{ secs}} \quad (26)$$

$$\text{Advertisement } I_{\text{avg}} = 1.235 \text{ mA} \times \frac{86400 - (30 \times 24)}{0.5 \text{ sec}} \times .0099 \text{ sec} \times \frac{1}{24 \text{ hrs}} \times \frac{1}{60 \text{ mins}} \times \frac{1}{60 \text{ secs}} \quad (27)$$

$$\text{Advertisement } I_{\text{avg}} = 0.024249 \text{ mA}$$

8.5.4 Average Standby Current

The standby current was measured as the average current consumption between each Bluetooth low energy advertisement pulse. Therefore, to solve the amount of time the smart lock is in standby mode, subtract the amount of times the lock is in other states from the total time (see Equation 28). Then, multiply the standby current by the percentage of total time it is in standby mode (see Equation 30). The measured standby current is 4.7 μ A.

$$\text{Standby Time} = 24 \text{ hrs} \times 60 \text{ mins} \times 60 \text{ secs} - \text{Number of BLE Advertisement Pulses} \times \text{Pulse Duration} - \text{Number of BLE Connected Pulses} \times \text{Events} \times \text{Connected Pulse Duration} \quad (28)$$

The connected time includes the time that the lock is in the motor and LED state.

$$\text{Time in Standby} = 86400 \text{ secs} - \frac{86400 - (\text{Connected Time} \times \text{Events})}{\text{Advertising Period}} \times \text{Pulse Duration} - \frac{\text{Connected Time} - \text{Motor Event Time}}{\text{Connection Period}} \times \text{Connected Pulse Duration} \times \text{Events} \quad (29)$$

$$\text{Standby } I_{\text{avg}} = 0.0047 \text{ mA} \times \left(86400 \text{ secs} - \frac{86400 \text{ secs} - (30 \text{ secs} \times \text{Events})}{0.5 \text{ secs}} \times 0.0099 \text{ secs} - \frac{30 \text{ secs} - 2 \text{ secs}}{0.03 \text{ secs}} \times 0.0076 \times \text{Events} \times \frac{1}{24 \text{ hrs}} \times \frac{1}{60 \text{ mins}} \times \frac{1}{60 \text{ secs}} \right) \quad (30)$$

$$\text{Standby } I_{\text{avg}} = 0.004598 \text{ mA}$$

8.5.5 Estimated Battery Life

The total system average current must be found to accurately estimate battery life. The total average current is found by adding each of the average currents (see [Table 7](#) and [Equation 31](#)).

Table 7. Current Consumption per State

STATE	AVERAGE CURRENT (µA)
Motor and LEDs	27.8 µA
Bluetooth low energy connected	1.6 µA
Bluetooth low energy advertisement	24.2 µA
Standby	4.6 µA
Total average current	58.2 µA

$$\text{Battery Life in Years} = \frac{\text{Battery Capacity (mAh)}}{\text{Avg Current (mA)}} \times \frac{1}{(8760 \text{ hr / yr})} \times \text{Derating Factor} \tag{31}$$

The derating factor in [Equation 31](#) accounts for self-aging of the battery.

$$\text{Battery Life in Years} = \frac{3000 \text{ mAh}}{0.058178 \text{ mA}} \times \frac{1}{(8760 \text{ hr / yr})} \times 0.90 \tag{32}$$

[Figure 54](#) shows a comparison of the experimental and theoretical battery life of the TIDA-00757 reference design. The theoretical has less battery life because more assumptions were made regarding motor current, standby current, and power topology losses. The theoretical estimated current consumption for each state was much higher than what was actually measured in the experimental phase of testing.

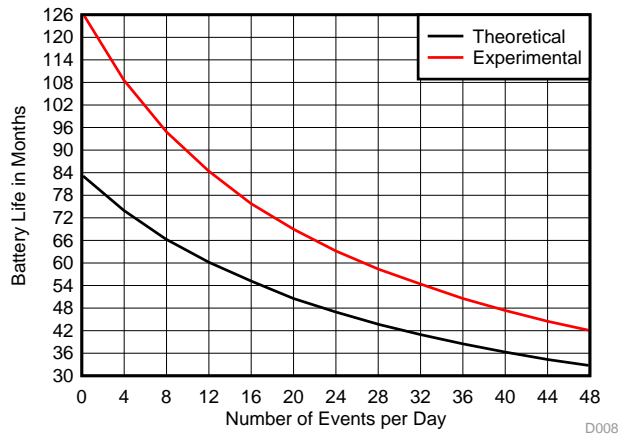


Figure 54. Number of Events Versus Battery Life (Theoretical and Experimental)

9 Design Files

9.1 Schematics

To download the schematics, see the design files at: [TIDA-00757](#).

9.2 Bill of Materials

To download the bill of materials, see the design files at [TIDA-00757](#).

9.3 PCB Layout Recommendations

To ensure high performance, the TIDA-00757 reference design was laid out using a 4-layer PCB. The second layer is a solid GND pour, and the third layer is used for power rail routing without a ground fill. The top and bottom layers are used for general signal routing and also have GND fills in unused areas. For all of the TI products used in this TI Design, adhere to the layout guidelines detailed in their respective data sheets. The onboard Bluetooth antenna was placed as far away from other noise sources as possible, such as the buck converter or other items that could act as an antenna (for example test points or large traces).

9.3.1 Layout Prints

To download the layer plots, see the design files at: [TIDA-00757](#).

9.4 Altium Project

To download the Altium project files, see the design files at: [TIDA-00757](#).

9.5 Layout Guidelines

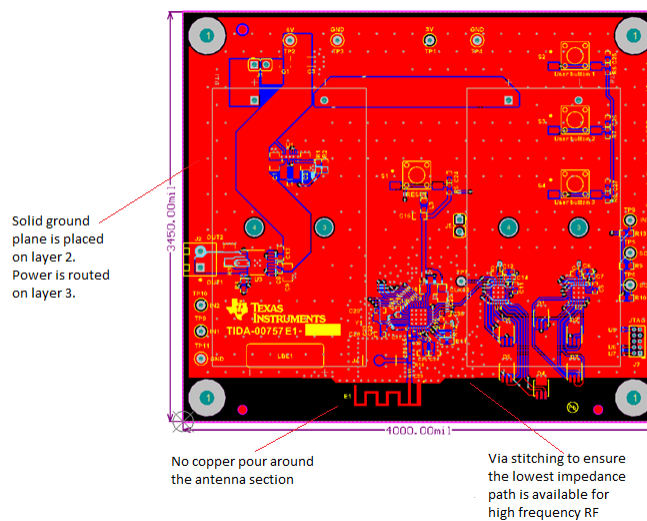


Figure 55. Smart Lock Reference Design Layout Guidelines

9.6 Gerber Files

To download the Gerber files, see the design files at: [TIDA-00757](#).

9.7 Assembly Drawings

To download the assembly drawings, see the design files at: [TIDA-00757](#).

10 Software Files

To download the software files, see the design files at: [TIDA-00757](#).

11 References

1. Texas Instruments, *Reverse Current Battery Protection Circuits*, Application Report ([SLVA139](#))
2. Texas Instruments, *Calculating Motor Driver Power Dissipation*, Application Report ([SLVA504](#))
3. Texas Instruments, WEBENCH Design Center, (<http://www.ti.com/webench>)

11.1 Trademarks

E2E, SimpleLink, SmartRF, Code Composer Studio, DCS-Control, MSP430 are trademarks of Texas Instruments.

WEBENCH is a registered trademark of Texas Instruments.

Cortex is a registered trademark of ARM.

HomeKit, LightBlue are trademarks of Apple, Inc.

Apple is a registered trademark of Apple, Inc.

Arm is a registered trademark of Arm Limited (or its subsidiaries).

Bluetooth is a registered trademark of Bluetooth SIG, Inc.

CoreMark is a registered trademark of Core-Mark International, Inc.

Energizer is a registered trademark of Energizer Holdings, Inc.

Android is a trademark of Google, Inc.

Samsung, Galaxy S are registered trademarks of Samsung Electronics Co., Ltd.

Tektronix is a registered trademark of Tektronix, Inc.

ZigBee is a registered trademark of ZigBee Alliance.

12 About the Authors

JARROD KREBS is a systems designer at Texas Instruments, where he is responsible for developing reference designs in the industrial segment. Jarrod has experience with software and embedded applications implemented on Arm-based microcontrollers and TI's MSP430™ platforms. Jarrod earned his bachelor of science in computer engineering from Kansas State University in Manhattan, KS. Jarrod is also a member of the Institute of Electrical and Electronics Engineers (IEEE).

ARAMIS P. ALVAREZ is a systems architect at Texas Instruments, where he is responsible for developing reference design solutions for the industrial segment. Aramis brings to this role experience in system-level analog, mixed-signal, power management, and board design. Aramis earned his master of science in electrical engineering (MSEE) degree from the University of Michigan-Ann Arbor, and earned a bachelor of science in electrical engineering (BSEE) degree from the University of Florida.

CHRISTINA S. LAM is a systems architect at Texas Instruments where she is responsible for developing firmware for reference design solutions in the industrial segment. Christina has broad experience with applications processors, microcontrollers, and digital-signal processors with specialties in embedded firmware. Christina earned her bachelor of science in electrical and computer engineering from the University of Texas at Austin.

Revision History

NOTE: Page numbers for previous revisions may differ from page numbers in the current version.

Changes from B Revision (January 2018) to C Revision Page

- Changed all instances of CC2640 to CC2640R2F 1

Changes from A Revision (October 2016) to B Revision Page

- Removed *Bluetooth*® Smart 2

Changes from Original (August 2016) to A Revision Page

- Deleted "Low Rx / Tx Current (6 mA / 9 mA)" from [Features](#) 1
- Deleted "Low $R_{DS(on)}$ of 360 mΩ from Motor Driver" from [Features](#) 1
- Added "Total Average Current Consumption of 58.2 μA (24 Locks and Unlocks Per Day)" to [Features](#) 1
- Added "4.6-μA Standby Current" to [Features](#) 1
- Deleted "DC-DC Converter Uses 71.1 μA of Average Power (220-ms Connection Interval)" from [Features](#)..... 1

IMPORTANT NOTICE FOR TI DESIGN INFORMATION AND RESOURCES

Texas Instruments Incorporated ("TI") technical, application or other design advice, services or information, including, but not limited to, reference designs and materials relating to evaluation modules, (collectively, "TI Resources") are intended to assist designers who are developing applications that incorporate TI products; by downloading, accessing or using any particular TI Resource in any way, you (individually or, if you are acting on behalf of a company, your company) agree to use it solely for this purpose and subject to the terms of this Notice.

TI's provision of TI Resources does not expand or otherwise alter TI's applicable published warranties or warranty disclaimers for TI products, and no additional obligations or liabilities arise from TI providing such TI Resources. TI reserves the right to make corrections, enhancements, improvements and other changes to its TI Resources.

You understand and agree that you remain responsible for using your independent analysis, evaluation and judgment in designing your applications and that you have full and exclusive responsibility to assure the safety of your applications and compliance of your applications (and of all TI products used in or for your applications) with all applicable regulations, laws and other applicable requirements. You represent that, with respect to your applications, you have all the necessary expertise to create and implement safeguards that (1) anticipate dangerous consequences of failures, (2) monitor failures and their consequences, and (3) lessen the likelihood of failures that might cause harm and take appropriate actions. You agree that prior to using or distributing any applications that include TI products, you will thoroughly test such applications and the functionality of such TI products as used in such applications. TI has not conducted any testing other than that specifically described in the published documentation for a particular TI Resource.

You are authorized to use, copy and modify any individual TI Resource only in connection with the development of applications that include the TI product(s) identified in such TI Resource. NO OTHER LICENSE, EXPRESS OR IMPLIED, BY ESTOPPEL OR OTHERWISE TO ANY OTHER TI INTELLECTUAL PROPERTY RIGHT, AND NO LICENSE TO ANY TECHNOLOGY OR INTELLECTUAL PROPERTY RIGHT OF TI OR ANY THIRD PARTY IS GRANTED HEREIN, including but not limited to any patent right, copyright, mask work right, or other intellectual property right relating to any combination, machine, or process in which TI products or services are used. Information regarding or referencing third-party products or services does not constitute a license to use such products or services, or a warranty or endorsement thereof. Use of TI Resources may require a license from a third party under the patents or other intellectual property of the third party, or a license from TI under the patents or other intellectual property of TI.

TI RESOURCES ARE PROVIDED "AS IS" AND WITH ALL FAULTS. TI DISCLAIMS ALL OTHER WARRANTIES OR REPRESENTATIONS, EXPRESS OR IMPLIED, REGARDING TI RESOURCES OR USE THEREOF, INCLUDING BUT NOT LIMITED TO ACCURACY OR COMPLETENESS, TITLE, ANY EPIDEMIC FAILURE WARRANTY AND ANY IMPLIED WARRANTIES OF MERCHANTABILITY, FITNESS FOR A PARTICULAR PURPOSE, AND NON-INFRINGEMENT OF ANY THIRD PARTY INTELLECTUAL PROPERTY RIGHTS.

TI SHALL NOT BE LIABLE FOR AND SHALL NOT DEFEND OR INDEMNIFY YOU AGAINST ANY CLAIM, INCLUDING BUT NOT LIMITED TO ANY INFRINGEMENT CLAIM THAT RELATES TO OR IS BASED ON ANY COMBINATION OF PRODUCTS EVEN IF DESCRIBED IN TI RESOURCES OR OTHERWISE. IN NO EVENT SHALL TI BE LIABLE FOR ANY ACTUAL, DIRECT, SPECIAL, COLLATERAL, INDIRECT, PUNITIVE, INCIDENTAL, CONSEQUENTIAL OR EXEMPLARY DAMAGES IN CONNECTION WITH OR ARISING OUT OF TI RESOURCES OR USE THEREOF, AND REGARDLESS OF WHETHER TI HAS BEEN ADVISED OF THE POSSIBILITY OF SUCH DAMAGES.

You agree to fully indemnify TI and its representatives against any damages, costs, losses, and/or liabilities arising out of your non-compliance with the terms and provisions of this Notice.

This Notice applies to TI Resources. Additional terms apply to the use and purchase of certain types of materials, TI products and services. These include; without limitation, TI's standard terms for semiconductor products (<http://www.ti.com/sc/docs/stdterms.htm>), [evaluation modules](#), and [samples](http://www.ti.com/sc/docs/sampterm.htm) (<http://www.ti.com/sc/docs/sampterm.htm>).

Mailing Address: Texas Instruments, Post Office Box 655303, Dallas, Texas 75265
Copyright © 2018, Texas Instruments Incorporated